The WalRK two-component system is essential for proper cell envelope biogenesis in *Clostridioides difficile*

Ute Müh,[1] Craig D. Ellermeier[1], David S. Weiss[1]

[1]Department of Microbiology and Immunology, University of Iowa, Iowa City, IA 52242

Corresponding authors: craig-ellermeier@uiowa.edu, david-weiss@uiowa.edu

Running title: WalRK is essential in *C. difficile*

Abstract (229 words)

The WalR-WalK two-component regulatory system (TCS) is found in all Firmicutes, where it regulates the expression of multiple genes required for remodeling the cell envelope during growth and division. Unlike most TCSs, WalRK is essential for viability, so it has attracted interest as a potential antibiotic target. Here we used overexpression of WalR and CRISPR interference to investigate the Wal system of *Clostridioides difficile*, a major cause of hospital-associated diarrhea in high-income countries. We confirmed the *wal* operon is essential and identified morphological defects and cell lysis as the major terminal phenotypes of altered *wal* expression. We also used RNA-seq to identify over 150 genes whose expression changes in response to WalR levels. This gene set is enriched in cell envelope genes and includes several predicted PG hydrolases and proteins that could regulate PG hydrolase activity. A distinct feature of the *C. difficile* cell envelope is the presence of an S-layer and we found WalR affects expression of several genes which encode S-layer proteins. An unexpected finding was that some Wal-associated phenotypic defects were inverted in comparison to what has been reported in other Firmicutes. For example, down-regulation of Wal signaling caused *C. difficile* cells to become longer rather than shorter, as in *Bacillus subtilis*. Likewise, down-regulation of Wal rendered *C. difficile* more sensitive to vancomycin, whereas reduced Wal activity is linked to increased vancomycin resistance in *Staphylococcus aureus*.

Importance (100 words)

The WalRK two-component system (TCS) is essential for coordinating synthesis and turnover of peptidoglycan in Firmicutes. Here we investigate the WalRK TCS in *Clostridioides difficile*, an important bacterial pathogen with an atypical cell envelope. We confirmed that WalRK is essential and regulates cell envelope biogenesis, although several of the phenotypic changes we observed were opposite to what has been reported in other Firmicutes. We also identified over 150 genes whose expression is controlled either directly or indirectly by WalR. Overall, our findings provide a foundation for future investigations of an important regulatory system and potential antibiotic target in *C. difficile*.

36 **Introduction**

37 To grow and divide, bacteria must thoroughly remodel their peptidoglycan (PG) sacculus, a large,
38 covalently closed macromolecule that surrounds the cell and provides protection against rupture due to
39 turgor pressure (1). How bacteria remodel the sacculus without making errors that lead to inadvertent
40 lysis is a question that has fascinated microbiologists for decades. The question is also of practical
41 significance because small molecules that undermine normal peptidoglycan biogenesis are among our
42 most effective antibiotics.

43 An important advance in our understanding of cell envelope biogenesis was made over twenty
44 years ago when Fabret and Hoch identified a *Bacillus subtilis* two-component system (TCS) that is
45 essential for viability (2). This TCS is now called the Wal system and is known to coordinate expression
46 of multiple cell envelope genes in the Firmicutes. WalRK is essential in all species studied so far,
47 including pathogens such as *Staphylococcus aureus* (3-5) and *Streptococcus pneumoniae* (6, 7).
48 Because of its essentiality, the Wal TCS has attracted interest as a potential antibiotic target.

49 The Wal TCS comprises the bifunctional kinase/phosphatase WalK together with its cognate
50 response regulator WalR. In addition, *wal* operons typically include genes for membrane proteins known
51 or presumed to modulate WalK activity, but the accessory proteins differ between organisms (8-10).
52 Recent evidence from *B. subtilis* indicates WalK activity is regulated by PG fragments generated by PG
53 hydrolases that open spaces to make room for elongation. These PG fragments bind to WalK's
54 extracellular Cache domain to modulate the phosphorylation state of WalR (11). Phosphorylated WalR
55 in turn binds to various promoters to activate or repress gene expression.

56 The number of genes in the WalR regulon ranges from about a dozen to over 100 (5, 12-16),
57 depending on the species, and only some of these genes are directly activated or repressed by WalR.
58 Although WalR regulons are diverse, they invariably include multiple proteins that contribute to proper
59 biogenesis of the cell envelope, especially PG hydrolases. Consistent with these themes, the phenotypic

60 defects elicited by artificial up- or down-regulation of WalRK signaling include abnormal cell shape, larger
61 cells, smaller cells, ghost cells (lysis), thicker PG, abnormal division septa and altered sensitivity to
62 antibiotics that target PG biogenesis (8-10). In *S. pneumoniae walRK* is essential because it activates
63 expression of an essential PG hydrolase, *pcsB* (6, 7). However, the essentiality of *walRK* in *B. subtilis*
64 and *S. aureus* is polygenic in nature, resulting from abnormal expression of multiple genes that are not
65 by themselves essential. In all three organisms, it is possible to bypass the *walRK* requirement by
66 constitutively expressing one or more Wal regulon PG hydrolases, sometimes in combination with
67 deleting genes for hydrolase inhibitors (6, 17, 18).

68 Here we studied the WalRK TCS in *Clostridioides difficile*, an anaerobic, spore-forming Firmicute
69 responsible for close to a quarter million hospitalizations and over 12,000 deaths per year in the United
70 States (19). Unlike the envelope of most Firmicutes in which *walRK* has been studied previously, the *C.*
71 *difficile* envelope has a proteinaceous S-layer whose assembly presumably must be coordinated with PG
72 synthesis (20-22). In addition, the PG itself is somewhat unusual (23). About 90% of the *N*-
73 acetylglucosamine is deacetylated (which has implications for PG hydrolase activity) and about 70% of
74 the peptide crosslinks are 3-3 rather than 4-3 (which has implications for the structure of PG fragments
75 thought to bind to the Cache domain of WalK (11)). The *C. difficile* Wal system includes a unique
76 lipoprotein gene and a non-canonical WalK that lacks an intracellular PER-ARNT-SIM (PAS) signaling
77 domain (Fig. 1) (10). These features distinguish *C. difficile's* WalRK TCS from those of previously
78 characterized Firmicutes, although a distantly related *wal*-like system in *Mycobacterium tuberculosis*
79 (MtrAB) includes a lipoprotein and a WalK-like histidine kinase without an intracellular PAS domain (10,
80 24, 25). Finally, our recent development of tools for xylose-inducible gene expression and CRISPR
81 interference (26) helped to overcome some of the challenges inherent in phenotypic analysis of essential
82 genes like *walRK* in *C. difficile*.

83

84

85 **Results**

86 **The *wal* operon is required for cell viability, proper rod morphology and intrinsic resistance to**
87 **some antibiotics.** According to Tn-seq, the WalRK TCS is essential in *C. difficile* (27). To confirm and
88 extend this finding, we leveraged the power of CRISPR interference (CRISPRi) for functional analysis of
89 essential genes/operons (28). Our CRISPRi system comprises a xylose-inducible nuclease-defective
90 Cas9, P_{xyl}::*dCas9*, that is targeted to a gene of interest by a single guide RNA expressed constitutively
91 from the glutamate dehydrogenase promoter, P_{gdh}::*sgRNA* (26). Because CRISPRi is polar, we decided
92 to target the first gene in the operon, which encodes a predicted lipoprotein unique to the *C. difficile wal*
93 operon (Fig. 1). We have named this gene *walA.* For reproducibility, we designed two guides against
94 *walA*, sgRNA-*walA1* and sgRNA-*walA2*. Subsequent RNA-seq experiments described below confirmed
95 that targeting dCas9 to *walA* suppressed transcription of the entire operon. As a negative control we used
96 a sgRNA (sgRNA-neg) that does not have a target anywhere on the *C. difficile* chromosome. In some
97 experiments the CRISPRi machinery was produced from a plasmid that confers resistance to
98 thiamphenicol (Thi), while in others it was integrated into the chromosome at the *pyrE* locus in a way that
99 does not leave behind an antibiotic resistance marker (29).

100 Chromosomal- or plasmid-based CRISPRi knockdown of the *wal* operon in either 630Δerm or
101 R20291 reduced viability $\geq 10^4$-fold when cell were plated on TY-agar containing 1% xylose (Fig. 2A and
102 Fig. S1A). Additional phenotypes were characterized in TY broth using 630Δerm derivatives with the
103 CRISPRi machinery integrated at *pyrE*. In the absence of xylose, sgRNA-*walA1* and sgRNA-*walA2*
104 retarded growth slightly compared to the sgRNA-neg control (Fig. 2B, S1B). This finding indicates there
105 is leaky expression of P_{xyl}::*dCas9,* which was later confirmed by RNA-seq (see below). Under these
106 conditions, cells were on average about 10% longer than wild-type and the fraction of cells with curved
107 or irregular contours increased from ~1% in the sgRNA-neg control to ~20% for sgRNA-*walA1* or ~10%
108 for sgRNA-*walA2* (Fig. 2C-E, S1E,F). Further knockdown of the *wal* operon by addition of xylose
109 exacerbated the growth defect in a dose-dependent manner (Fig. 2B, S1D). In addition, morphological

110 defects became more pronounced, with cells now averaging ~30% longer than controls and up to ~40%
111 exhibiting curved or irregular contours (Fig. 2D,E and S1E,F).

112 Partial knockdown of the *wal* operon in the absence of xylose allowed us to screen for altered
113 sensitivity to antibiotics that target cell envelope biogenesis. We found that the minimal inhibitory
114 concentration (MIC) for ampicillin and daptomycin decreased about 2-fold, while the MIC for vancomycin
115 decreased about 4-fold (Table 1). But sensitivity to the other two cell wall-active antibiotics, imipenem
116 and bacitracin, or the gyrase inhibitor novobiocin was not affected (Table 1).

117

118 **Overexpression of WalR impairs growth, alters morphology and slows autolysis**. We also
119 investigated Wal function in *C. difficile* by overproducing the response regulator WalR to drive cells into
120 an exacerbated Wal-ON state (5, 30). Plating *C. difficile* 630Δerm harboring a P_{xyl}::*walR* expression
121 plasmid onto TY-Thi containing 1% xylose resulted in a 10^6-fold loss of viability (Fig. 3A). This strain failed
122 to grow when subcultured directly into TY-Thi broth containing 1% xylose, but waiting until OD_{600} ~0.2
123 before adding 3% xylose resulted in only a subtle growth defect (Fig. 3B). Three hours post-induction,
124 the cells had become strikingly phase bright and resistant to autolysis when suspended in buffer
125 containing 0.01% Triton X-100 (Fig. 3C,D). Triton X-100 is thought to reduce the inhibitory effect of
126 lipoteichoic acids on PG hydrolases (31, 32). Similar results were obtained in the R20291 strain
127 background (Fig. S3). It is unclear what causes cells to turn phase bright upon overexpression of *walR*.
128 Differential staining with Syto 9 and propidium iodide (LIVE/DEAD staining) indicates that >99% of the
129 cells are alive after overproduction of WalR (Fig. 3B, red arrow).

130 We repeated these experiments after integrating P_{xyl}::*walR* into the chromosome of 630Δerm. As
131 expected, the effects of xylose induction were similar but less pronounced when P_{xyl}::*walR* was in single
132 copy (Fig. 4A). The addition of xylose at subculture was now tolerated and reduced growth in a dose-
133 dependent manner. At 3% xylose, cells became slightly phase-bright. There were some bent or hooked
134 cells, a defect not observed with the P_{xyl}::*walR* plasmid, perhaps because it could only be induced for

135 shorter times. (Fig. 4C). After 6h of induction, cells were harvested and evaluated in the lysis assay. We
136 found that overexpression of *walR* slowed lysis in a dose-dependent manner (Fig. 4B).

137 **Expression profiling under Wal-ON conditions.** As a step towards understanding the basis of the
138 various Wal-related phenotypes, we sought to identify the genes in the *wal* regulon. (Note: we use the
139 term regulon for convenience to refer to genes whose expression responds to manipulation of the *wal*
140 operon regardless of whether these effects are direct or indirect.) We began by performing RNA-seq on
141 two strains that overexpress *walR* from a single copy P_{xyl}::*walR* construct integrated at *pyrE*. One of these
142 strains overproduced wild-type WalR, the other overproduced a $WalR^{D54E}$ mutant protein expected to
143 mimic phosphorylated WalR and thus be constitutively active (13, 33) (Confusingly, D54 is annotated as
144 D66 in the R20291 genome on the BioCyc website). The two strains behaved similarly with respect to
145 growth and performance in the lysis assay (Fig. S4A,B). The control strain for these experiments had the
146 gene for a red fluorescent protein (*rfp*) integrated at *pyrE* (26). Strains were grown overnight in TY, then
147 subcultured into fresh TY at a starting OD_{600} ~0.05. When the OD_{600} reached ~0.2, cultures were induced
148 with 3% xylose and allowed to grow for three hours (~ 2 mass doublings), at which time cells were
149 harvested and processed for RNA-seq. At this time point induction of *walR* had only a small effect on
150 growth rate (Fig. S4A) and >99% were viable as judged by LIVE/DEAD staining.

151 Not including *walR*, which was induced directly from P_{xyl}, the RNA-seq analysis identified 77
152 genes whose transcript abundance changed ≥4-fold ($p<0.05$) upon overexpression of either *walR* or
153 $walR^{D54E}$ (Table 2). Of these genes, 44 were induced and 33 were repressed. Induction ratios were very
154 similar in the *walR* and $walR^{D54E}$ strains with only two exceptions, *cd630_03901* and *cd630_10631*, both
155 of which encode hypothetical proteins. The failure of the D54E substitution to increase gene expression
156 could mean it is not activating in *C. difficile* WalR, as reported previously for some other response
157 regulators (34). Alternatively, overexpression of *walR* is itself activating and might obscure the effects of
158 the substitution. The 77 genes are predicted by BioCyc (35) to be organized into 65 operons that contain
159 18 additional genes which missed our 4-fold expression change cut-off. Visual inspection of the
160 expression data revealed these genes almost always trended in the right direction, confirming the

161 predicted structure of most of the operons. We therefore included these 18 genes in what we will refer to
162 as the Wal-ON regulon, bringing it to a total of 95 genes in 65 operons (Table 2).

163 Several of the genes and trends in Table 2 are worth highlighting. Xylose induction resulted in a
164 14-fold increase in *walR* mRNA (13-fold for *walR*^{D54E}), while the levels of *walK* or other members of the
165 native operon were not affected. This means that induction of P_{xyl}::*walR* integrated at *pyrE* does not lead
166 to induction of the native *wal* operon, consistent with reports that the *wal* operon is not auto-regulated in
167 other bacteria (8, 16). Another striking feature of Table 2 is the abundance of genes encoding for cell
168 envelope proteins. Of the 95 genes in Table 2, 22 (23%) are predicted to encode exported proteins and
169 29 (31%) are predicted to encode cytoplasmic membrane proteins. For comparison, ~7% of the entire
170 proteome is predicted to be exported and 23% predicted to be membrane proteins (see Methods). Table
171 2 also includes 21 hypotheticals (22% of the total), many of which are likely to be involved in cell envelope
172 processes based on the presence of predicted transmembrane domains or export signals.

173 Peptidoglycan-associated genes, especially PG hydrolases, are prominent members of the Wal
174 regulon in all Firmicutes examined to date (8, 10), and *C. difficile* is no exception. Table 2 lists ten
175 peptidoglycan-associated genes, including the second most highly induced gene, *pgdA*, which was
176 upregulated 16-fold. PgdA deacetylates N-acetylglucosamine in peptidoglycan, and is important for *C.*
177 *difficile's* high lysozyme resistance (36, 37). AsnB (~8-fold induced) is annotated as an asparagine
178 synthetase, but its primary function is to amidate diaminopimelic acid in PG stem peptides (38). In *B.*
179 *subtilis*, amidation of m-DAP inhibits PG hydrolase activity (39). MurE (7-fold repressed) catalyzes one
180 of the cytoplasmic steps in PG synthesis, addition of diaminopimelic acid to the nucleotide-linked PG
181 precursor (40). Down regulation of *murE* suggests PG synthesis may be decreased in Wal-ON conditions.
182 Cwp16 and Cwp17 are S-layer proteins with predicted amidase domains (41) and were upregulated
183 about 4-fold. Cell wall amidases cleave the amide bond that links stem peptides to N-acetylglucosamine
184 in PG glycan strands (42). CD630_36010 (4-fold induced) is a predicted D-alanyl-D-alanine
185 carboxypeptidase that removes the terminal D-Ala moiety from peptidoglycan pentapeptide sidechains.
186 This might limit 4-3 crosslinking of stem peptides, but could favor 3-3 crosslinking. Two proteins of

187 unknown function were upregulated >10-fold, CD630_07390 and CD630_07380. We suspect both of
188 these proteins are involved in PG metabolism because they are predicted to be exported and also
189 induced by lysozyme (43). Notable among the repressed genes in Wal-ON cells is *cd630_27680*, which
190 is down regulated about 4-fold and predicted to encode a cell wall hydrolase from the NlpC/P60 family,
191 a domain common to endopeptidases (42). Interestingly, this gene is preceded by two putative WalR
192 binding sites, and it has also been characterized as a sortase substrate (44). Another predicted PG
193 hydrolase, CD630_23880, is mildly repressed (~3-fold). Interestingly, this gene is cotranscribed with an
194 uncharacterized BlaI-BlaR regulatory system, *cd630_23890* and *cd630_23900*. Some BlaIR regulatory
195 systems respond to beta-lactam stress (45, 46).

196 One of the questions that motivated this study was whether the WalR system regulates genes for
197 S-layer proteins in *C. difficile*. Indeed, the Wal-ON regulon includes six S-layer protein genes, all of which
198 are upregulated by WalR: *cwp2*, *5*, *12*, *16*, *17* and *66*. Two of these genes were mentioned already, the
199 cell wall amidases *cwp16* and *cwp17*. The remaining four are of unknown function, although *cwp2* and
200 *cwp12* have domains implicated in adhesion or pathogenesis, and studies with *cwp66* have linked it to
201 adhesion, autolysis and resistance to antibiotics (41, 47). WalRK has been suggested to regulate an S-
202 layer gene in *Bacillus anthracis* (48).

203

204 **Expression profiling under Wal-OFF conditions.** As a complementary approach to identify genes in
205 the WalR regulon, we assessed the effect of CRISPRi knockdown of the *wal* operon on global gene
206 expression. To this end, we performed RNA-seq on a 630Δerm derivative that has the CRISPRi
207 machinery (P_{xyl}::*dCas9*, P_{gdh}::*sgRNA-walA1*) integrated into the chromosome at *pyrE*. The control strain
208 was identical except that it expressed an innocuous sgRNA that does not target anywhere in the *C.*
209 *difficile* genome (P_{gdh}::*sgRNA*-neg). Two induction conditions were used. One of these, called "no xylose",
210 relied on leaky expression of *dCas9*. For this, overnight cultures were diluted into fresh TY to a starting
211 OD_{600} = 0.03 and harvested when they reached OD_{600} ~0.7 (Fig. S4C). For the other condition, called
212 "low xylose", cultures in exponential growth where induced with 0.1% xylose at an OD_{600} = 0.1 and

213 incubated 2.5 hours (~2 mass doublings) before harvest. This induction regimen reduced cell density
214 only modestly (Fig. S4D).

215 There are 49 genes, organized in 27 operons that shift 4-fold or more under Wal-OFF conditions
216 (Table 3). The 27 operons contain an additional 14 genes that did not meet our 4-fold cut-off, all but three
217 of which nevertheless trended in the right direction. The three exceptions include a pseudogene
218 (*cd630_05260*) that is not detected by our RNA-seq analysis tool and two membrane proteins
219 (*cd630_05290* and *05280*) whose expression was unchanged. Thus, for the purposes of this analysis,
220 CRISPRi knockdown of the *wal* operon changed the expression of 60 genes, of which 44 were induced
221 and 16 were repressed. Curiously, for most of these genes the fold-change was larger in the absence of
222 xylose, suggesting that many of the effects on gene expression might be indirect.

223 The CRISPRi guide targets the first gene in the operon, *walA*, which was repressed 6.8-fold in
224 the absence of xylose and 35-fold with low xylose. As expected, polarity resulted in repression of the
225 downstream genes as well, ~5-fold with leaky CRISPRi, increasing to ~15-fold with low xylose. The
226 observed polarity confirms the predicted operon structure, including that a seemingly unrelated (and
227 according to Tn-seq nonessential) gene for a tRNA modification enzyme is indeed part of the operon.

228 Unexpectedly, the Wal-OFF gene set comprises mostly transporters and genes for various
229 metabolic functions. Not counting the members of the *wal* operon, only one of the genes is predicted to
230 be exported and 15 genes (25%) to be membrane proteins, a percentage comparable to the genome as
231 a whole (Methods). Remarkably, the Wal-OFF regulon does not include a single annotated PG
232 metabolism gene. However, we observed ~5-fold repression of the *dltDABC* operon, which is responsible
233 for the addition of D-alanine to teichoic acids (49). We identified a predicted WalR binding site
234 immediately upstream of *dltDABC*, suggesting direct regulation by WalR. This putative WalR binding site
235 had previously been recognized as one of two direct repeat sequences in the *dlt* promoter region ((49),
236 Table S4). D-alanylation of teichoic acids affects PG hydrolase activity (50, 51) and vancomycin
237 resistance in some bacteria (52, 53). In *C. difficile*, a *dltD* insertion mutant is sensitized to vancomycin
238 and some antimicrobial peptides, but the effects are <2-fold (52). Only one gene in Table 3 codes for an

239 S-layer protein—the hemagglutinin/adhesin *cwpV*, which was ~16-fold induced in no xylose. But this
240 gene is subject to phase variation (54), leading us to suspect it may not be a true member of the WalR
241 regulon.
242
243 **Comparison of the Wal-ON and the Wal-OFF gene sets reveals little overlap but opposing trends.**
244 There are only two proteins common to the Wal-ON and the Wal-OFF gene sets, *cd630_20160*
245 (hypothetical protein) and *cd630_28620* (annotated as a membrane peptidase). However, a large fraction
246 of the 79 Wal-ON genes that met the 4-fold cut-off trend in the opposite direction when evaluated under
247 Wal-OFF conditions, even though the magnitude of change is not as large (Fig. 5A, Table 2). A similar
248 observation was made when genes affected 4-fold or more under Wal-OFF conditions were examined
249 under Wal-ON conditions (Fig. 5B, Table 3).
250
251 **Select members of the WalR regulon were confirmed by plasmid-based reporter fusions**. To
252 confirm results of the RNA-seq analysis, we constructed *rfp* transcriptional fusions (55) to the promoter
253 regions for seven genes from the Wal-ON or Wal-OFF gene sets. Four genes were chosen primarily
254 because they were highly-induced when WalR was overexpressed: *cd630_07390*, *pgdA*, *cd630_07380*,
255 and *cd630_08670* (Table 2). Additional considerations included that *pgdA* has an obvious connection to
256 PG biogenesis (36, 37), while *cd630_08670* has a predicted WalR-binding site (Table S4). Two genes
257 were chosen because they were the most strongly repressed upon CRISPRi knockdown of the *wal*
258 operon and are preceded by a predicted WalR-binding site: *cd630_28620* and *cd630_05300* (Tables 3,
259 S4). In addition, *cd630_28620* is one of only two genes that made the 4-fold cut-off in both Wal-ON and
260 Wal-OFF conditions. The final gene chosen for confirmation with an *rfp* reporter was *dltD*, which
261 incorporates D-alanine into teichoic acids (49) and was modestly downregulated by CRISPRi knockdown
262 of the *wal* operon. *dltD* stood out because it has a predicted WalR-binding site and is one of the few cell
263 envelope-associated genes that was at least 4-fold repressed in Wal-OFF conditions (Tables 3, S4).

264 Reporter plasmids were constructed by PCR-amplifying ~300 bp upstream of the start codon for
265 each selected gene. These fragments contain transcriptional start sites for five of the seven genes (Clost-
266 Base database (56)); start sites for the remaining two genes have not been mapped. The PCR products
267 were cloned into an RFP reporter plasmid. The resulting plasmids were conjugated into the appropriate
268 Wal-ON and Wal-OFF strain pairs: 630Δerm versus 630Δerm P_{xyl}*::walR* and 630Δerm with sgRNA-*walA1*
269 versus 630Δerm sgRNA-neg, respectively. Reporter strains were grown under the same conditions as
270 used for the RNA-seq experiments, except that the Wal-OFF condition was limited to growth in the
271 absence of xylose, i.e., assaying the effect of leaky dCas9 expression on the reporter gene. Harvested
272 cells were fixed and transferred to aerobic conditions to allow RFP to mature. Fluorescence was
273 quantified by flow cytometry.

274 We found that all RFP reporters responded in the expected direction when *walR* expression was
275 manipulated, thus confirming the RNA-seq results by an orthogonal method (Fig. 6). However, the fold
276 changes were uniformly about 4-fold greater by RNA-seq than by RFP fluorescence. The reasons for this
277 difference are not known. As an aside, having RNA-seq and RFP fluorescence data for the same genes
278 enabled us to show these are correlated, i.e., baseline RFP fluorescence was higher for genes that
279 returned more reads in RNA-seq experiments (Fig. S5A). This correlation was expected and further
280 indicates our RNA-seq data are robust.

281

282 **Altering the expression level of select regulon genes does not induce the *wal* reporter.** In *B.*
283 *subtilis*, the WalR regulon can be induced or repressed by manipulating expression of *walR*-regulated
284 genes involved in PG metabolism (11, 57). We therefore asked whether manipulating expression of *wal*
285 regulon genes in *C. difficile* would induce or repress expression of a chromosomal P_{cd630_07390}*::rfp*
286 reporter. The reporter was chosen because this promoter was highly induced in Wal-ON conditions as
287 determined by RNA-seq (38-fold) or a plasmid-based RFP reporter fusion (7-fold). The chromosomal
288 P_{cd630_07390}*::rfp* reporter was validated by confirming ~10-fold increased red fluorescence upon
289 overexpression of *walR* from a P_{xyl} plasmid (Fig. S5B). Next, we introduced a panel of plasmids that

290 allowed us to directly target 13 WalR regulon genes by overexpression and/or CRISPRi. These 13 genes
291 were chosen for various reasons including large fold-changes in expression, relevance to cell wall
292 biogenesis, and the presence of WalR binding sites (Table S3). Of note, the gene set included a putative
293 cell wall amidase and the predicted PG hydrolase with a NlpC/P60 domain. Unfortunately, neither
294 overexpression nor CRISPRi knockdown of the selected *wal* regulon genes altered expression of the
295 P_{cd630_07390}::*rfp* reporter. Further work will be needed to determine whether these negative results reflect
296 technical difficulties or more fundamental differences in Wal signaling between *B. subtilis* and *C. difficile*.
297

298 **Perturbation of select Wal regulon genes individually does not lead to any Wal-associated**
299 **phenotypic defects.** As noted above, one motivation for determining the Wal regulon was to identify
300 genes that contribute to Wal phenotypes. Recall that induction of P_{xyl}::*walR* decreases viability, causes
301 cells to become phase bright and reduces autolysis in buffer containing 0.01% Triton X-100 (Fig. 3). Two
302 of the most highly induced genes in Wal-ON conditions encode the hypothetical proteins CD630_07380
303 and CD630_07390. However, overproduction of these proteins either individually or from P_{xyl} plasmids
304 did not result in any obvious phenotypic changes (Fig. 7). Note, because these genes are transcribed
305 divergently (35), we needed to reverse the direction of one gene to express them together and decided
306 to clone both possible arrangements: *cd630_07380-cd630_07390* and *cd630_07390-cd630_07380*.
307 Likewise, a CRISPRi plasmid with an sgRNA that targets *cd630_27680* had no effects on growth,
308 morphology or lysis (Fig. 7); this gene encodes PG hydrolase with two predicted WalR-binding sites and
309 is among the most strongly repressed genes in Wal-ON conditions.

310 CRISPRi silencing of the *wal* operon is lethal, and the terminal phenotypes include lysis and loss
311 of rod shape as reflected by an abundance of curved cells (Fig. 2). However, none of these phenotypes
312 were observed when we used a P_{xyl}::*cwpV* plasmid to overexpress the most highly-induced gene from
313 the Wal-OFF RNA-seq data set, which we tested even though *cwpV* is subject to phase-variation and
314 might not be part of the WalR regulon. We also observed an effect when we used CRISPRi to knock
315 down expression of *dltD*, which was among the more strongly repressed Wal-OFF genes and is preceded

316 by a putative WalR binding site (Fig. 8). While not an exhaustive evaluation of all regulon members, our
317 findings suggest the phenotypic defects observed upon perturbation of the Wal system are not due to
318 changes in expression of any single gene, but cumulative in nature much like what has been observed
319 in *B. subtilis* and *S. aureus* (8-10, 12).
320

321 **Discussion**

322 In *C. difficile* the WalRK TCS is predicted to reside in a four gene operon: *walA-walR-walK-truA2*.
323 We altered expression of the WalRK regulon by complementary approaches: depleting *C. difficile* of
324 WalRK by CRISPRi knockdown of the entire operon, and overproduction of WalR under P_{xyl} control. RNA-
325 seq revealed the *wal* operon is not autoregulated in *C. difficile*, as evidenced by a lack of induction when
326 WalR (or $WalR^{D54E}$) was ectopically expressed from a P_{xyl} promoter. Wal operons are not autoregulated
327 in other Firmicutes either. RNA-seq also confirmed the genes constitute an operon, because CRISPRi
328 targeting *walA* resulted in roughly equivalent knockdown of the three downstream genes. Further studies
329 will be needed to establish the specific role of each gene in WalRK signaling. We suspect *walA* is a bona
330 fide part of the Wal system because all *wal* operons studied to date include accessory genes for
331 membrane proteins that modulate WalK signaling (8, 10). But a rationale for why a non-essential tRNA
332 modification enzyme, *truA2,* should have come to reside in the *wal* operon is not obvious. This might be
333 the result of evolutionary happenstance.

334 As expected, extensive knockdown of the *wal* operon with CRISPRi or strong overproduction of
335 WalR from a P_{xyl} plasmid were both lethal. Phenotypic defects depended on how *walRK* expression was
336 manipulated, but included elongation, loss of rod shape (curved or wavy cells), phase bright cells,
337 enhanced or reduced autolysis, and altered sensitivity to antibiotics that target PG synthesis. Similar
338 phenotypes have been observed upon manipulating Wal signaling in other organisms (2, 6, 7, 9, 10, 12,
339 17, 18). But there are some intriguing differences. In *B. subtilis*, where phosphorylated WalR promotes
340 elongation, artificial upregulation of the Wal system causes cells to become elongated while artificial

341 downregulation causes cells to become short (10, 18). In *C. difficile*, however, overexpression of WalR
342 from P_{xyl} had no obvious effect on cell length while CRISPRi knockdown of the *wal* operon led to
343 elongation.

344 Vancomycin resistance presents another example of an inverse phenotype. In *S. aureus* down
345 regulating *walRK* expression increases resistance to vancomycin while up regulation of *walRK* decreases
346 vancomycin resistance (58, 59). Vancomycin-intermediate *S. aureus* (VISA) strains, both laboratory
347 derived (60) or isolated in the clinic (61), often have mutations in *walR* or *walK* that down regulate the
348 system (62). In contrast, we found that partial CRISPRi knockdown of the *wal* operon in *C. difficile* had
349 the opposite effect, namely, a modest increase in sensitivity to vancomycin. Vancomycin is a front line
350 treatment for *C. difficile* infections, so our findings suggest a small molecule that interferes with Wal
351 signaling might enhance the efficacy of vancomycin therapy.

352 RNA-seq identified over 150 genes whose expression responds to manipulation of Wal signaling
353 in *C. difficile*. Although this gene set is diverse, there are themes: many cell envelope proteins, many
354 hypotheticals, and about 10 proteins with various connections to PG metabolism. There are also 7 genes
355 for S-layer proteins, consistent with the need to coordinate S-layer assembly and remodeling with growth
356 and turnover of the PG sacculus. The PG hydrolases are of particular interest because they are prominent
357 members of the WalR regulon in other Firmicutes (5, 12-16) and ectopic expression of one or more of
358 these enzymes can render *walRK* no longer essential regulators (6, 17, 18). In *C. difficile*, Wal-ON
359 conditions induced two putative cell wall amidases (*cwp16*, *cwp17*) and repressed one potential D,L-
360 endopeptidase (*cd630_27680*). Direct control of *cd630_27680* by WalR is suggested by the presence of
361 two matches to the WalR binding site consensus sequence about 100 nucleotides upstream of the start
362 codon (Table S4). The importance of these genes for any Wal-related phenotypes is unclear, however,
363 because overexpression and CRISPRi knockdown experiments did not result in any phenotypic changes
364 or alter expression of an RFP reporter that is induced under Wal-ON conditions. In addition to the putative
365 hydrolases, several genes in the WalR regulon may play a role in *controlling* PG hydrolase activity.

366 Deacetylation of PG N-acetylglucosamine (GlcNAc) (63), mDAP amidation (39), and D-alanylation of
367 teichoic acids (32, 50, 51, 64) have all been shown to affect hydrolase activity in other organisms.

368 *S. pneumoniae* is so far the only organism in which a single essential gene, the PG hydrolase
369 *pcsB*, has been identified to be responsible for the essentiality of the *wal* system (6, 7). In *B. subtilis*,
370 essentiality of the Wal system arises from the cumulative impact of aberrant expression of multiple genes
371 involved in turnover of PG (5, 10, 11). Wal essentiality is also polygenic in nature in *S. aureus* (8). This
372 seems to be the case in *C. difficile* as well. Although CRISPRi silencing of the *wal* operon leads to cell
373 lysis, the Wal-OFF gene set (Table 3) does not include any genes determined to be essential by
374 transposon mutagenesis (27). In contrast, the Wal-ON regulon (Table 2) includes 3 essential genes. Two
375 of these are induced by WalR, DNA ligase (*ligA, cd630_33090*) and a putative Calcium-chelating protein
376 (*cd630_26810*); one is repressed, the PG precursor synthesis protein MurE (*cd630_26640*). It is possible
377 that repression of *murE* contributes to death during overexpression of WalR, but not during CRISPRi
378 knockdown of the *wal* operon, because *murE* expression did not change under that condition. Overall,
379 our findings suggest essentiality of WalRK is driven by a deleterious imbalance of multiple processes.
380 (As an aside, it is worth noting that repression of *murE* under Wal-ON conditions is not what one would
381 expect if WalR promotes increased PG synthesis, as in *B. subtilis* (11, 57)).

382 Here we have provided an initial delineation of Wal phenotypes and the WalR regulon in *C.*
383 *difficile*. Our findings raise a number of exciting questions. Is the protein WalA involved in WalRK
384 signaling, and if so, how? What signals are sensed by WalK? Of note, owing to differences in crosslinking
385 (23), the PG hydrolysis products implicated in regulating WalK activity in *B. subtilis* (11) are not very
386 abundant in *C. difficile*. Moreover, *C. difficile* WalK is missing an intracellular PAS domain found in most
387 other WalK proteins, suggesting *C. difficile* WalK senses different signals and/or transmits those signals
388 differently. Another open question is which WalR regulon genes are controlled directly by WalR. It will
389 also be important to determine the functions of the WalR regulated genes, especially the many

390 hypothetical proteins. Answers to these questions are likely to provide novel insights into cell wall
391 biogenesis and might point the way towards improved therapies against this important pathogen.

392

393 **Methods**

394 **Strains, media, and growth conditions.** Bacterial strains are listed in Table 4. *C. difficile* strains used
395 in this study were derived from either 630Δerm or R20291, both of which have been sequenced. *C.*
396 *difficile* was routinely grown in tryptone-yeast extract (TY) medium, supplemented as needed with
397 thiamphenicol at 10 µg/ml (TY-Thi). TY medium consisted of 3% tryptone, 2% yeast extract, and 2% agar
398 (for plates). Brian heart infusion (BHI) media was prepared per manufacturer's (DIFCO) instructions. *C.*
399 *difficile* strains were maintained at 37°C in an anaerobic chamber (Coy Laboratory Products) in an
400 atmosphere of 10% H_2, 5% CO_2, and 85% N_2. *Escherichia coli* strains were grown in LB medium at 37°C
401 with chloramphenicol at 10 µg/ml or ampicillin at 100 µg/ml as needed. LB medium contained 1%
402 tryptone, 0.5% yeast extract, 0.5% NaCl, and 1.5% agar (for plates). OD_{600} measurements were made
403 with the WPA Biowave CO8000 tube reader in the anaerobic chamber.

404

405 **Plasmid and strain construction**. All plasmids are listed in Table 5; an expanded version of this table
406 which includes additional information relevant to plasmid assembly is provided in Table S2A in the
407 supplemental material. Plasmids were constructed by isothermal assembly (65) using reagents from New
408 England Biolabs (Ipswich, MA). Regions of plasmids constructed using PCR were verified by DNA
409 sequencing. The oligonucleotide primers used in this work were synthesized by Integrated DNA
410 Technologies (Coralville, IA) and are listed in Table S2B. All plasmids were propagated using OmniMax
411 2-T1R as the cloning host, transformed into HB101/pRK24 (66, 67), and then introduced into *C. difficile*
412 strains by conjugation. Chromosomal fusions at the *pyrE* locus in 630Δerm were constructed by allelic
413 exchange (29) using *C. difficile* CRG1496 (630Δ*erm* Δ*pyrE*) as a *pyrE*-deficient recipient. The allelic
414 exchange restored a functional *pyrE* gene.

415

416 **Conjugation into *C. difficile.*** Our experiments required conjugating plasmids into *C. difficile*
417 strains R20291 and 630Δerm. In the case of R20291 we encountered problems with low conjugation
418 efficiencies even with heat shock as described (68). After testing several modifications of the procedure,
419 we found that performing conjugations on filters reliably increased efficiency more than 10-fold (Fig. S6).
420 We now routinely use filters for all our conjugations. Briefly, the *E. coli* donor strain (an HB101/pRK24
421 derivative harboring the cargo plasmid) was grown overnight in LB Amp^{100} Cam^{10}. The donor strain was
422 collected gently by centrifugation of a 0.5 ml aliquot at 5000 x g for 1 min, then washed with 1 ml TY and
423 pelleted again. The washed cell pellet was moved into the anaerobic chamber. R20291 was prepared for
424 conjugation by a heat shock step (68). For this, a 200 µl aliquot of the overnight culture of the R20291
425 recipient was transferred to a 1.5 ml microfuge tube and incubated at 48°C for 5 min in a Fisherbrand
426 Dry bath (with water-filled wells). Then 100 µl of heat-shocked R20291 was used to take up the pellet of
427 *E. coli* donor cells. The strain mixture was then pipetted on to a 25 mm diameter, 0.45 µm pore size
428 Millipore mixed cellulose filter (HAWP02500) placed on brain heart infusion (BHI) plates. After incubation
429 for 24 h at 37°C, cells were flushed from the membrane with 500 µL TY and 200-500 µL of the resulting
430 bacterial slurry was plated on TY amended with thiamphenicol (10 µg/ml), kanamycin (50 µg/ml) and
431 cefoxitin (8 µg/ml) to select for exconjugants. Conjugations into 630Δerm were done identically except
432 the heat shock step was omitted.

433

434 **Viability assay.** The effect of CRISPRi silencing on plating efficiency was evaluated by making a 10-fold
435 serial dilution of a culture grown overnight in TY Thi10 and spotting 5 µl of each dilution on TY Thi10 agar
436 with and without 1% xylose. Plates were photographed after overnight incubation (~18 h).

437

438 **Microscopy.** Cells were immobilized using thin agarose pads (1%). Phase-contrast and fluorescent
439 micrographs were recorded on an Olympus BX60 microscope equipped with a 100× UPlanApo objective
440 (numerical aperture, 1.35). Micrographs were captured with a Hamamatsu Orca Flash 4.0 V2+

441 complementary metal oxide semiconductor (CMOS) camera. The image analysis tool MicrobeJ (69) was
442 used to measure cell length and sinuosity, which is the length of the cell axis divided by the distance
443 between the poles. A perfectly straight rod has a sinuosity value of 1, while a curved or wavy cell has a
444 larger value. We classified cells as curved if their sinuosity was ≥1.03 (see Fig. S2 for examples). Viability
445 of cells was assessed with LIVE/DEAD stain (Molecular Probes L7012). A 1 mL culture sample was
446 pelleted, washed with PBS and resuspended in 100 µL PBS with 5 µM Syto 9 and 30 µM propidium
447 iodide. Cells were incubated with the dyes for 15 min, then removed from the anaerobic chamber and
448 immediately imaged by microscopy. For propidium iodide red fluorescence we used filter set 41004
449 (Chroma Technology) with a 538 to 582-nm excitation filter, 595-nm dichroic mirror (long pass), and a
450 582 to 682-nm emission filter. Syto 9 green fluorescence was captured with filter set 41017 (Chroma
451 Technology Corp) with a 450- to 490-nm excitation filter, a 495-nm dichroic mirror (long pass), and a 500-
452 to 550-nm emission filter.
453
454 **Fixation protocol.** A 500-µl aliquot of cells in growth medium was added directly to a microcentrifuge
455 tube containing 120 µl of a 5x fixation cocktail: 100 µl of a 16% (wt/vol) paraformaldehyde aqueous
456 solution (Alfa Aesar, Ward Hill, MA) and 20 µl of 1 M $NaPO_4$ buffer (pH 7.4). The sample was mixed,
457 incubated in the anaerobic chamber at 37°C for 30 min, then on ice 30 min, and removed from the
458 chamber. The fixed cells were washed twice with 1 mL phosphate-buffered saline (PBS), resuspended
459 in 50 µl of PBS, and left in the dark for 18 h to allow for chromophore maturation.
460
461 **MIC determination.** Antibiotic sensitivity was determined in 96 well plates. A twofold dilution series of
462 select antibiotics was prepared in 50 µl TY medium. Wells were then inoculated with 50 µl of a diluted
463 culture suspension (10^6 CFU/ml; calculated OD_{600} ~0.005). Plates were imaged and evaluated after 17h
464 at 37°C.
465

466 **Lysis assay.** Cell cultures (1 mL) were removed from the anaerobic chamber, pelleted and resuspended
467 in 700 µL 0.01% Triton X-100 in 50 mM $NaPO_4$ buffer (pH 7.4). Of this 700 µL, three 200 µL replicates
468 were pipetted into wells of a clear, flat bottom 96-well plate. The turbidity was measured at 600 nm every
469 15 min for 10 h in a plate reader (Tecan Infinite M200 Pro).
470
471 **Flow cytometry.** Cells were analyzed at the Flow Cytometry Facility at the University of Iowa using the
472 Becton, Dickinson LSR II instrument with a 561-nm laser, a 610/20-nm-band-pass filter, and a 600 LP
473 dichroic filter. Data were analyzed using BD FACSDiva software.
474
475 **Culture growth for RNA-seq samples**. To achieve robust, quality data all experiments were performed
476 on three different days for biological replicates. Cultures were grown in 100 mL TY as follows. Wal-ON:
477 to characterize the effect of overexpressing *walR*, strains were subcultured to OD_{600} ~0.05, grown to 0.2,
478 induced with xylose to 3% and grown for an additional 3h (Fig. S4A). Wal-OFF: to characterize the effect
479 of partial knockdown of the *wal* operon under leaky CRISPRi conditions, strains were subcultured to
480 OD_{600} ~0.03 and grown to ~0.7 before harvesting (Fig. S4C). To test the effect of stronger knockdown of
481 the *wal* operon, growth conditions were identified that allowed exposing cells to moderate levels of xylose
482 (0.1%) without a significant loss of biomass. Strains were subcultured to OD_{600} ~0.03, grown to 0.3,
483 diluted back to ~0.1 and induced with xylose to a final concentration of 0.1% and harvested after an
484 additional 2.5 h of growth (Fig. S4D). From each condition, 25 mL culture was fixed by rapidly mixing with
485 25 mL ice-cold 1:1 ethanol:acetone that had been brought into the anaerobic chamber on dry ice. Fixed
486 cells were stored at -80°C until further workup.
487
488 **RNA isolation and RNA-Seq.** Fixed culture samples were thawed, pelleted for 10 min at 8000 x g, 4°C
489 and pellets washed once with 500 µL 1% β-mercaptoethanol (β-ME) in water. Subsequent steps are an
490 adaptation of the Qiagen RNeasy Mini Kit procedure. The washed pellet was resuspended in 1 mL of the
491 Qiagen-provided RTL buffer amended with 1% β-ME and transferred to a 2 mL screwcap tube filled with

492 glass beads (0.1 mm diameter) to a height of ~2-3 mm. Cells were lysed with the FastPrep-24
493 homogenizer with two cycles at 6m/s for 45 s, resting on ice for 3 min between cycles. The homogenized
494 material was pelleted at 14,000 x g for 15 min at 4°C. The supernatant was removed, adjusted to 900 µL
495 with RTL/β-ME, mixed with 500 µL ethanol and loaded onto the Qiagen RNeasy spin column. Subsequent
496 steps followed the manufacturer's protocol. The RNA was eluted with 50 µL water and DNase treated
497 twice (Ambion Turbo DNA-free). Absence of DNA was evaluated by amplifying a 364 bp region of *mldA*
498 with Taq DNA polymerase for 30 cycles. The RNA integrity number (RIN) was determined with an Agilent
499 Bioanalyzer at the Iowa Institute for Human Genetics, Genomics Division. All samples had a RIN of 9.4
500 or higher. Typical yields from 25 mL culture were 8-20 µg RNA at 200-500 ng/µL.

501 RNA samples were submitted to the Microbial Genome Sequencing Center (MiGS) in Pittsburgh,
502 PA. MiGS performed Illumina Stranded RNA library preparation paired with RiboZero Plus (per
503 manufacturer's specifications) and sequenced on a NextSeq 500 using a 75cyc High Output flowcell.
504 Fastq files were trimmed and filtered using a combination of Trimmomatic (70) and FastQC
505 (https://www.bioinformatics.babraham.ac.uk/projects/fastqc/). Alignment, normalization and differential
506 expression was analyzed with SeqMan NGen® Version 17.2. DNASTAR, Madison, WI. Annotation was
507 imported from NCBI with additional information obtained from progenomes (71). All subsequent analysis
508 was performed in Excel and GraphPad Prism 9.

509

510 **Bioinformatics**. Gene sequences and operon organization were obtained from the BioCyc data
511 collection (35, 72). SignalP 5.0 (73) was used to search for Type I and Type II signal peptides. BUSCA
512 (74) was used to predict protein cellular location. When all *C. difficile* proteins were run through the
513 prediction programs, SignalP predicted ~7% to be exported. BUSCA predicted ~4% to exported and
514 ~25% to be membrane associated. Cell wall association in Tables 2 and 3 was reported as follows: (i)
515 signal peptidase substrate if predicted by SignalP; (ii) for all remaining genes: membrane protein if
516 predicted by BUSCA.

517 Putative WalR binding sites were identified with Virtual Footprint (75) by querying with (1) the *B.*
518 *subtilis* consensus motif, TGTWAH-N5-TGTWAH (14), (2) the same motif, but allowing one mismatch, or
519 (3) TGTNDH-N5-BKBWRN (8). Searches were limited to the intergenic region of the genome and
520 generated 29, 522, and 684 hits respectively.

521

522 **Data availability**

523 RNA-seq data were submitted to the NCBI GEO repository and assigned accession number GSE200346.

524

525 **Acknowledgements**

526 This work was supported by National Institutes of Health grants R01AI087834 (CDE) and
527 R01AI155492 (CDE and DSW) from the National Institutes for Allergy and Infectious Disease. Cell
528 fluorescence was quantitated at the Flow Cytometry Facility, which is a Carver College of Medicine /
529 Holden Comprehensive Cancer Center core research facility at the University of Iowa. The facility is
530 funded through user fees and the generous financial support of the Carver College of Medicine, Holden
531 Comprehensive Cancer Center, and Iowa City Veteran's Administration Medical Center. RNA integrity
532 was characterized by the Genomics Division of the Iowa Institute of Human Genetics which is supported,
533 in part, by the University of Iowa Carver College of Medicine. We thank Nigel Minton for pMTL-YN1C,
534 Brianne Zbylicki for plasmid pBZ101, and members of the Ellermeier and Weiss laboratories for helpful
535 discussions.

536

537

538 **Table 1.** Effect of CRISPRi-silencing *wal* on sensitivity to antibiotics[a]

	MIC [µg/mL]		
	sgRNA-neg	sgRNA-*walA1*	sgRNA-*walA2*
Ampicillin	6.3	3.5	3.1
Imipenem	3.1	3.1	2.6
Vancomycin	4.6	0.9	0.7
Daptomycin	11.3	4.1	5.7
Bacitracin	250	250	250
Novobiocin	13	17	16

539 [a]Results are the average of measurements done in duplicate on four different days.

540 **Table 2. Genes affected by Wal-ON conditions.**

541

Gene, changed ≥ 4-fold	Operon[1]	Gene name	Annotation	Log$_2$ fold change			Cell wall association[3]
				WalR overexpression		CRISPRi against *wal*[2]	
				WalR	WalR^{D54E}		
cd630_07390	07390		hypothetical protein	5.26	5.70	-1.38	SPI
cd630_15220	15220	*pgdA*	peptidoglycan deacetylase	4.02	4.26	-1.09	SPI
cd630_05490	05490		hypothetical protein	3.87	4.51	-1.84	SPI
	17810	*walA*	lipoprotein	nc[4]	nc	-2.76	SPII
cd630_17820	17820	*walR*	TC response regulator	3.81	3.67	-2.51	
	17830	*walK*	TC sensor histidine kinase	nc	nc	-2.33	Membrane
	17840	*truA2*	tRNA pseudouridine synthase A	nc	nc	-2.34	
cd630_07380	07380		hypothetical protein	3.43	4.14	-1.22	SPI
cd630_08670	08670		hypothetical protein	3.28	3.97	nc	Membrane
cd630_07400	07400		PLP dependent aminotransferase	3.21	2.38	nc	
cd630_10880	10880		hypothetical protein	2.88	3.14	-1.40	Membrane
cd630_01660	01660		peptidase	2.76	2.95	nc	
	01650		amino acid transporter	nc	nc	nc	Membrane
cd630_27940	27940	*cwp12*	cell wall binding protein	2.69	2.82	nc	SPI
cd630_33090	33090	*ligA*	DNA ligase	2.64	2.62	nc	
cd630_18250	18250	*metY*	O-acetylhomoserine sulfhydrylase	2.50	2.80	-0.57	
cd630_18260	18260	*metA*	homoserine O-succinyltransferase	2.60	2.85	-0.88	
cd630_14281	14281		hypothetical protein	2.59	3.22	nc	
cd630_27860	27860	*cwp5*	cell wall binding protein	2.51	2.65	nc	SPI
cd630_25380	25380		lipoprotein	2.47	2.70	-0.70	SPII
cd630_03910	03910	*asnB*	asparagine synthetase	2.47	3.30	nc	Membrane
cd630_14960	14960		hypothetical protein	2.37	2.86	-0.74	SPI
cd630_25370	25370		5'-nucleotidase/phosphoesterase	2.33	2.49	-0.59	SPI
cd630_27910	27910	*cwp2*	cell wall binding protein	2.30	2.36	-0.59	SPI
	27900		LmbE-like deacetylase	1.56	1.46	-0.55	
	27890	*cwp66*	cell wall binding protein	1.41	1.42	-0.58	SPI
cd630_28620	28620		peptidase	2.29	2.24	-2.53	
cd630_34880	34880	*gtaB1*	UTP-G1P uridylyltransferase	2.23	2.34	-0.73	
cd630_20580	20580		hypothetical protein	2.22	2.43	-1.26	Membrane
cd630_07410	07410	*glpK1*	glycerol kinase	2.21	0.63	nc	
	07420	*eutH*	ethanolamine utilization protein	1.46	nc	nc	Membrane
	10350	*cwp16*	amidase, cell wall binding protein	1.24	1.33	nc	SPI
cd630_10360	10360	*cwp17*	amidase, cell wall binding protein	2.15	2.35	nc	SPI
cd630_21170	21170	*trxB2*	thioredoxin reductase	2.12	2.18	nc	
cd630_00210	00210	*pycA*	pyruvate carboxylase	2.10	2.16	-0.46	
cd630_13890	13890		chloromuconate cycloisomerase	2.09	2.18	-0.28	
	13900		hypothetical protein	1.30	1.64		Membrane
cd630_22490	22490		ATPase	2.07	2.20	nc	

Gene, changed ≥ 4-fold	Operon[1]	Gene name	Annotation	Log$_2$ fold change			Cell wall association[3]
				WalR overexpression		CRISPRi against *wal*[2]	
				WalR	WalR^{D54E}		
cd630_22480	22480		hypothetical protein	1.81	2.04	nc	
cd630_10890	10890	*rgbR*	TC response regulator	2.04	2.24	-1.13	
	10900	*rgbS*	TC sensor HK (fragment)	nc	1.16	nc	Membrane
cd630_30930	30930		aminobutyrate hydrolase	2.15	2.35	nc	
	30920		putative amino acid transporter	1.52	1.02	nc	Membrane
cd630_26810	26810		putat. Ca-chelating protein	2.01	2.59	nc	SPI
cd630_36010	36010		D-Alanyl-D-alanine carboxypeptidase	1.99	2.35	-1.38	SPI
cd630_00220	00220		Elongation factor G	1.97	2.09	nc	
cd630_14290	14290		Acyl-CoA N-acyltransferase	1.92	2.47	-1.15	
cd630_22280	22280		Hypothetical protein	1.83	2.05	-0.70	Membrane
cd630_01100	01100		Hypothetical protein	1.81	2.02	nc	Membrane
	01110		Hypothetical protein	1.51	1.73	nc	SPI
	01111		Hypothetical protein	nc	1.14	nc	
cd630_09940	09940		Serine-pyruvate aminotransferase	1.77	2.10	nc	
cd630_19942	19942		Hypothetical protein	1.74	2.12	nc	
cd630_05270	05270		Beta-lactamase-like hydrolase	1.73	2.13	-0.85	
cd630_22270	22270		Radical SAM protein	1.67	2.02	-0.55	SPII
cd630_18070	18070		NADPH-dependent FMN reductase	1.49	2.07	-1.53	Membrane
cd630_03901	03901		Hypothetical protein	0.92	2.37	nc	
cd630_10631	10631		Hypothetical protein	-0.07	2.18	-0.62	Membrane
cd630_30360	30360		Major facilitator superfamily transporter	-1.59	-2.13	1.11	Membrane
cd630_10540	10540	*bcd2*	Acyl-CoA dehydrogenase	-1.93	-2.23	1.03	
cd630_10550	10550	*etfB*	Electron transfer flavoprotein beta	-1.78	-2.11	1.07	
cd630_10560	10560	*etfA*	Electron transfer flavoprotein alpha	-1.95	-2.18	1.10	
cd630_10570	10570	*crt2*	3-Hydroxybutyryl-CoA dehydratase	-1.96	-2.27	1.06	
cd630_31000	31000		C4-dicarboxylate anaerobic carrier	-1.88	-2.59	nc	Membrane
cd630_30990	30990		Amidohydrolase	-1.80	-2.47	nc	Membrane
cd630_10580	10580	*hbd*	3-Hydroxybutyryl-CoA dehydrogenase	-1.86	-2.05	0.89	SPII
cd630_10590	10590	*thlA1*	Acetyl-CoA acetyltransferase	-1.96	-2.16	0.77	
	16820	*queK*	Queuosine hydrolase monomer	-1.31	-1.60	nc	
	16830		ECF transporter S-comp.	-1.39	-1.65	nc	Membrane
cd630_16840	16840	*queL*	Radical SAM superfamily protein	-1.90	-2.06	nc	
	23900		BlaI-like	-1.47	-1.65	nc	
cd630_23890	23890		BlaR-like	-1.94	-2.26	0.80	Membrane
	23880		Putat. PG hydrolase	-1.50	-1.77	nc	SPI
	36040		Hypothetical protein	-0.86	-0.94	0.71	
cd630_36030	36030		Phosphoesterase	-1.97	-2.01	1.09	Membrane
cd630_14040	14040		Oligopeptide transporter	-2.02	-2.03	nc	Membrane
	14041		Hypothetical protein	-2.02	-1.88	nc	
	25120		PTS, subunit IIA	-1.11	-1.47	nc	
	25110		PTS, antiterminator	-1.45	-1.46	nc	
cd630_25100	25100		PTS, subunit IIBC	-2.04	-2.19	0.97	Membrane

Gene, changed ≥ 4-fold	Operon[1]	Gene name	Annotation	Log$_2$ fold change			Cell wall association[3]
				WalR overexpression		CRISPRi against *wal*[2]	
				WalR	WalR^{D54E}		
cd630_25320	25320		Alanine-glyoxylate transaminase	-2.05	-2.34	1.41	
cd630_25310	25310		Hypothetical protein	-2.67	-2.75	1.35	Membrane
cd630_27680	27680		Cell-wall hydrolase	-2.06	-2.29	nc	SPI
cd630_29660	29660	*adhE1*	Acetaldehyde-CoA/alcohol dehydrogenase	-2.08	-2.37	-1.09	Membrane
cd630_18120	18120		Response regulator	-2.08	-2.28	nc	
cd630_22600	22600		Major facilitator superfamily transporter	-2.13	-2.32	nc	Membrane
cd630_20160	20160		Hypothetical protein	-2.19	-2.29	4.18	
cd630_25090	25090		Glycoside hydrolase	-2.22	-2.33	1.16	
cd630_21070	21070		Permease family protein	-2.23	-2.32	nc	Membrane
cd630_10220	10220		YczE-like membrane protein	-2.26	-2.73	0.93	Membrane
	10230		Transcriptional regulator	-1.70	-1.94	1.63	
cd630_10240	10240	*potA*	ABC transport ATP-binding protein	-2.27	-2.36	1.77	
cd630_10250	10250	*potB*	ABC transport permease	-2.47	-2.82	1.72	Membrane
cd630_10260	10260	*potC*	ABC transport permease	-2.53	-2.39	1.60	Membrane
cd630_10270	10270	*potD*	ABC transport substrate binding protein	-2.29	-2.37	1.55	SPII
cd630_26640	26640	*murE*	UDP-N-acetylmuramoylalanyl-D-glutamate-2, 6-diaminopimelate ligase	-2.85	-3.07	0.93	
cd630_26670	26670	*ptsG-BC*	PTS, subunit IIBC	-3.17	-3.52	nc	SPI
cd630_26660	26660	*ptsG-A*	PTS, subunit IIA	-3.12	-3.51	nc	
cd630_21510	21510		Hypothetical protein	-3.56	-3.82	0.68	Membrane

[1] Lists other operon members in order

[2] CRISPRi against *wal*: Fold change comparing sgRNA-neg to sgRNA-*walA1* strain in the absence of xylose

[3] Reports predictions by SignalP (SPI, predicted to be a substrate of signal peptidase I; SPII, predicted to be a substrate of signal peptidase II) and by BUSCA (membrane). The BUSCA prediction is only given for those genes that were not already predicted to be SPI or SPII substrates by SignalP.

[4] nc: no change, i.e. the fold change was close to 1 and the P-value >0.05

Abbreviations: TC (two component), PTS (phosphoenolpyruvate-dependent sugar phosphotransferase system)

552 **Table 3** Genes affected by Wal-OFF conditions

553

Gene, changed ≥ 4-fold	Operon[1]	Gene name	Annotation	Log$_2$ fold change			Cell wall association[3]
				CRISPRi		WalR OE[2]	
				No xyl	Low xyl		
cd630_05140	05140	*cwpV*	Hemagglutinin/adhesin	4.69	2.74	nc[4]	SPI
cd630_20160	20160		Hypothetical protein	4.18	1.65	-2.19	
cd630_11700	11700		Hypothetical protein	3.52	1.83	nc	
cd630_11710	11710	*etfB4*	Electron transfer flavoprotein alpha	3.30	1.40	nc	
cd630_11720	11720	*etfA4*	Electron transfer flavoprotein alpha	2.58	1.24	nc	
cd630_11730	11730		FAD-linked oxidase	2.17	1.08	nc	
cd630_08320	08320	*aksA*	Trans-homoaconitate synthase	3.11	2.02	nc	
cd630_08330	08330	*acnB*	Aconitate hydratase	3.06	2.05	nc	
cd630_08340	08340	*icd*	Isocitrate dehydrogenase	3.07	2.16	nc	
cd630_17290	17290		Sodium:phosphate symporter	2.76	0.45	-1.46	Membrane
cd630_13840	13840		LamB/YcsF family protein	2.17	0.88	nc	
cd630_13850	13850		Hypothetical protein	2.36	1.15	nc	Membrane
cd630_13860	13860		Allophanate hydrolase subunit 1	2.52	1.28	nc	
cd630_13870	13870		Allophanate hydrolase subunit 2	2.60	1.14	nc	
cd630_24260	24260	*buk1*	Butyrate kinase	2.45	nc	-1.41	
	24250	*ptb2*	Phosphate butyryltransferase	1.65	nc		
cd630_24240	24240		Pyridoxal phosphate-dependent transferase	2.55	nc	-1.15	
	24230		Putative transporter	1.17	nc		Membrane
cd630_07650	07650	*srlEa*	PTS, IIB N-terminal component	2.17	nc	nc	
cd630_07660	07660	*srlEb*	PTS, IIB C-terminal component	2.29	nc	nc	Membrane
cd630_07670	07670	*srlB*	PTS, IIA subunit	2.27	nc	nc	
cd630_07680	07680	*srlD*	Sorbitol-6-phosphate dehydrogenase	2.35	nc	nc	
	00350		Transcriptional regulator	1.46	0.55	-0.86	
cd630_00360	00360	*acoA*	Acetoin dehydrogenase E1 alpha	2.20	0.94	nc	
cd630_00370	00370	*acoB*	Acetoin dehydrogenase E1 beta	2.29	0.91	nc	
cd630_00380	00380	*acoC*	Acetoin dehydrogenase E2	2.20	0.72	nc	
cd630_00390	00390	*acoL*	Acetoin dehydrogenase E3	2.04	0.83	-0.57	
cd630_30010	30010		Hydrolase/isomerase/hydratase	2.25	nc	nc	
cd630_23920	23920		tRNA-binding protein	2.15	1.65	-1.77	
cd630_30960	30960	*bglA3*	6-Phospho-beta-glucosidase	2.13	nc	nc	
cd630_30950	30950	*bglA2*	6-Phospho-beta-glucosidase	2.07	nc	nc	
cd630_25150	25150		Aspartate aminotransferase	2.12	2.38	-1.76	

Gene, changed ≥ 4-fold	Operon[1]	Gene name	Annotation	Log$_2$ fold change			Cell wall association[3]
				CRISPRi		WalR OE[2]	
				No xyl	Low xyl		
	24291		Flavo/ferredoxin oxidoreductase delta	1.19	nc	nc	
cd630_24290	24290		Flavo/ferredoxin oxidoreductase alpha	2.11	nc	-0.91	
	24280		Flavo/ferredoxin oxidoreductase beta	1.66	nc	nc	
	24270		Flavo/ferredoxin oxidoreductase gamma	1.50	nc	nc	
cd630_30040	30040	*kdgT2*	2-Keto-3-deoxygluconate permease	2.08	0.33	0.93	Membrane
cd630_30020	30020	*uxaA*	D-galactate dehydratase/altronate hydrolase	2.06	0.25	nc	
cd630_32630	32630	*pstC*	Phosphate ABC transporter, PstC	2.03	nc	nc	Membrane
	32620	*pstA*	Phosphate ABC transporter, PstA	1.03	nc	nc	Membrane
	32610	*pstB*	Phosphate ABC transporter, ATP binding	1.80	nc	nc	
	32600	*phoU*	Phosphate uptake regulator	1.25	nc	nx	
	30980	*bglG1*	PTS, antiterminator	0.95	nc	nc	
cd630_30970	30970	*bglF2*	PTS, subunit IIABC	2.01	nc	-0.76	Membrane
cd630_28540	28540	*dltD*	D-alanine transferase	-1.52	-2.41	1.03	Membrane
cd630_28530	28530	*dltA*	D-ala-D-ala carrier protein ligase 1	-1.34	-2.27	0.84	
cd630_28520	28520	*dltB*	D-alanyl transferase	-1.34	-2.23	0.49	Membrane
	28510	*dltC*	D-ala-D-ala carrier protein ligase 2	-1.27	-1.89	nc	
cd630_09000	09000	*opuCA*	ABC transporter ATP-binding protein	-1.69	-2.36	1.46	
cd630_09010	09010	*opuCC*	ABC transporter permease	-1.68	-2.40	1.27	Membrane
cd630_05190	05190		Hypothetical protein	-2.00	-2.59	0.57	Membrane
	05260		Aminobenzoyl-glutamate transporter	nd[5]	nd	nd	
cd630_05250	05250		Peptidase	-2.15	-1.08	nc	
cd630_17671	17671		Hypothetical protein	-2.18	-1.99	nc	
cd630_17680	17680		Membrane protein	-2.23	-2.18	0.56	Membrane
cd630_17810	17810	*walA*	Lipoprotein	-2.76	-5.14	nc	SPII
cd630_17820	17820	*walR*	TC response regulator	-2.51	-3.91	3.81	
cd630_17830	17830	*walK*	TC sensor histidine kinase	-2.33	-4.03	nc	Membrane
cd630_17840	17840	*truA2*	tRNA pseudouridine synthase A	-2.34	-3.92	nc	
cd630_05300	05300		Membrane protein	-2.47	nc	nc	Membrane
	05290		Membrane protein	nc	nc	nc	Membrane
	05280		Amidohydrolase	nc	nc	0.92	
cd630_28620	28620		Peptidase	-2.53	-1.43	2.29	

[1] Lists other operon members in order

[2] Fold change comparing WalR overexpression to negative control strain

557 [3] Predictions by SignalP (SPI, predicted to be a substrate of signal peptidase I; SPII, predicted to be a
558 substrate of signal peptidase II) and by BUSCA (membrane). The BUSCA prediction is only given for
559 those genes that were not already predicted to be SPI or SPII substrates by SignalP.
560 [4] nc: no change, i.e. the fold change was close to 1 and the P-value >0.05
561 [5] nd: CD630_05260 is a pseudogene that was not detected by the RNA-seq analysis tool
562 Abbreviations: TC (two component), PTS (phosphoenolpyruvate-dependent sugar phosphotransferase
563 system)
564

565 **Table 4** Strains used in this study

566

Strain	Genotype and/or description	Source or reference
E. coli		
OmniMAX-2 T1^R	F′ [*proAB*$^+$ *lacI*^{q} *lacZ*Δ M15 Tn*10*(Tet^R) Δ(*ccdAB*)] *mcrA* Δ(*mrr-hsdRMS-mcrBC*) φ80(*lacZ*)ΔM15 Δ(*lacZYA-argF*) *U169 endA1 recA1 supE44 thi-1 gyrA96 relA1 tonA panD*	Invitrogen
HB101/pRK24	F− *mcrB mrr hsdS20*(r_B^- m_B^-) *recA13 leuB6 ara-14 proA2 lacY1 galK2 xyl-5 mtl-1 rpsL20*	(66, 67)
C. difficile		
R20291	Wild-type *C. difficile strain* from UK outbreak (ribotype 027)	
630Δ*erm*	Spontaneous erythromycin-sensitive derivative of strain 630 (ribotype 012)	(76)
CRG1496	630Δ*erm*Δ*pyrE*	(29)
UM275	630Δ*erm* with P_{veg}::*rfp* downstream of *pyrE*	(26)
UM554	630Δ*erm* with P_{xyl}::*dCas9* P_{gdh}::*sgRNA*-neg downstream of *pyrE*	This study
UM555	630Δ*erm* with P_{xyl}::*dCas9* P_{gdh}::*sgRNA-walA-1* downstream of *pyrE*	This study
UM556	630Δ*erm* with P_{xyl}::*dCas9* P_{gdh}::*sgRNA-walA-2* downstream of *pyrE*	This study
UM626	630Δ*erm* with P_{xyl}::*walR* downstream of *pyrE*	This study
UM628	630Δ*erm* with P_{xyl}::*walR*^{D54E} downstream of *pyrE*	This study
UM926	630Δ*erm* with P_{cd630_0739}::*mCherryOpt* downstream of *pyrE*	This study

567

568

569 **Table 5.** Plasmids used in this study

570

Plasmid	Relevant features	Reference or comment
pAP114	P_{xyl}::*mCherryOpt catP*	(26)
pBZ101	P_{xyl} empty vector	This study
pCE636	P_{dltD}::*mCherryOpt catP*	This study
pCE738	P_{xyl}::*dCas9-opt* P_{gdh}::*sgRNA-dltD-1 catP*	(37)
pCE691	P_{xyl}::*walR catP*	This study
pCE738	P_{xyl}::*dCas9-opt* P_{gdh}::*sgRNA-dltD-1 catP*	(37)
pCE741	P_{xyl}::*cdr2656*	This study
pCE744	P_{xyl}::*dCas9-opt* P_{gdh}::*sgRNA-cd630_27680-1 catP*	This study
pCE745	P_{xyl}::*dCas9-opt* P_{gdh}::*sgRNA-cd630_27680-2 catP*	This study
pCE789	P_{xyl}::*dCas9-opt* P_{gdh}::*cwpV-1 catP*	This study
pCE791	P_{xyl}::*cwpV*	This study
pDSW1728	P_{tet}::*mCherryOpt catP*	(55)
pDSW2037	P_{xyl} in integration vector pMTL-YN1C *catP*	This study
pDSW2053	P_{xyl}::*dCas9opt-*P_{gdh}::*sgRNA-neg* in pMTL-YN1C *catP*	This study
pDSW2055	P_{xyl}::*dCas9opt-*P_{gdh}::*sgRNA-cd630_17810-1* in pMTL-YN1C *catP*	This study
pDSW2057	P_{xyl}::*dCas9opt-*P_{gdh}::*sgRNA-cd630_17810-2* in pMTL-YN1C *catP*	This study
pIA33	P_{xyl}::*dCas9-opt* P_{gdh}::*sgRNA-rfp catP*	(26)
pIA34	P_{xyl}::*dCas9-opt* P_{gdh}::*sgRNA-neg catP*	(26)
pIA50	P_{xyl}::*dCas9-opt* P_{gdh}::*sgRNA-walA-1 catP*	This study
pIA51	P_{xyl}::*dCas9-opt* P_{gdh}::*sgRNA-walA-2 catP*	This study
pIA75	P_{xyl}::*walR* in pMTL-YN1C *catP*	This study
pIA76	P_{xyl}:*walR*^{D54E} in pMTL-YN1C *catP*	This study
pIA79	P_{xyl}::*dCas9-opt* P_{gdh}::*cd630_25040-1 catP*	This study
pIA80	P_{xyl}::*dCas9-opt* P_{gdh}::*cd630_25040-2 catP*	This study
pIA81	P_{xyl}::*dCas9-opt* P_{gdh}::*cd630_36010-1 catP*	This study
pIA93	P_{cdr_0665}::*mCherryOpt catP*	This study; *cdr_0665* is ortholog of *cd630_07380*

pIA95	P_{cdr_0796}::*mCherryOpt catP*	This study; *cdr_0796* is ortholog of *cd630_08670*
pIA97	P_{cdr_2753}::*mCherryOpt catP*	This study; *cdr_2753* is ortholog of *cd630_28620*
pIA98	P_{cdr_0455}::*mCherryOpt catP*	This study; *cdr_0455* is ortholog of *cd630_53000*
pIA100	P_{cd630_0739}::*mCherryOpt catP*	This study
pIA101	P_{cd630_0739}::*mCherryOpt* in pMTL-YN1C *catP*	This stduy
pIA102	P_{xyl}::*dCas9-opt* P_{gdh}::*cd630_05490 catP*	This study
pIA103	P_{xyl}::*dCas9-opt* P_{gdh}::*cd630_27940 catP*	This study
pIA104	P_{xyl}::*dCas9-opt* P_{gdh}::*cd630_27860 catP*	This study
pIA105	P_{xyl}::*dCas9-opt* P_{gdh}::*cd630_27910 catP*	This study
pIA106	P_{xyl}::*dCas9-opt* P_{gdh}::*cd630_10360 catP*	This study
pIA107	P_{pgdA}::*mCherryOpt catP*	This study
pIA108	P_{xyl}::*dCas9-opt* P_{gdh}::*cd630_07380-1 catP*	This study
pIA109	P_{xyl}::*dCas9-opt* P_{gdh}::*cd630_07380-2 catP*	This study
pIA110	P_{xyl}::*dCas9-opt* P_{gdh}::*cd630_07390-1 catP*	This study
pIA111	P_{xyl}::*dCas9-opt* P_{gdh}::*cd630_07390-2 catP*	This study
pIA112	P_{xyl}::*cd630_0738*	This study
pIA113	P_{xyl}::*cd630_0739*	This study
pIA114	P_{xyl}::*cd630_0738-cd630_0739*	This study
pIA115	P_{xyl}::*cd630_0739-cd630_0738*	This study
pMTL-YN1C	*E. coli-C. difficile* shuttle vector for inserting genes into *C. difficile* chromosome while restoring *pyrE*; *colE1 RP4oriT-TraJ CB102ori-repH' catP*	(29)

571

572

573

574

575 **Legends**

576 **Fig. 1. The *wal* operon of *C. difficile*.** Based on studies in other bacteria, WalK (red) is a bifunctional
577 signal transducing enzyme that can phosphorylate or dephosphorylate WalR (green). WalK is predicted
578 to have an extracellular Cache domain, as well as intracellular HAMP, HisKA (phospho-acceptor), and
579 HATPase domains. Unlike the *B. subtilis* ortholog (inset), it does not have an intracellular PAS domain.
580 WalR~P binds DNA to activate or repress expression of Wal-regulated genes. The lipoprotein (WalA,
581 blue), which is unique to *C. difficile*, may modulate WalK activity and is predicted to have a beta-propeller
582 lyase domain. The *truA2* gene codes for a pseudouridylate synthase and is not thought to play a role in
583 Wal signaling. Operon locus: *cdr20291_1676-1679* in R20291 and *cd630_17810-17840* in 630Δerm.

584

585 **Fig. 2. The *wal* operon is required for viability and normal rod morphology of *C. difficile* 630Δerm.**
586 (A) Viability assay. Serial dilutions of overnight cultures were spotted onto TY plates with or without 1%
587 xylose to induce the expression of *dCas9*. Plates were photographed after incubation overnight. Strains
588 carry chromosomal copies of the CRISPRi components and the following guides: sgRNA-neg (UM554),
589 sgRNA-*walA1* (UM555), and sgRNA-*walA2* (UM556). (B) Growth curves in liquid TY containing 0, 0.01,
590 0.1 or 1% xylose as indicated. For clarity, the sgRNA-neg control strain is graphed only at 0 xylose.
591 Samples were taken at 4 hours (arrow) for phase contrast microscopy (C), cell length measurements (D)
592 and determination of curvature (E). Numbers at the bottom of micrographs in (C) refer to % xylose. Note
593 cell debris indicative of lysis at 1% xylose. Bar = 10 μm. Cell length and percent curved cells were based
594 on about 500 cells per condition. The sgRNA-*walA1* strain is longer than the sgRNA-neg control in all
595 pairwise comparisons as determined by a T-test, $p<0.0001$.

596

597 **Fig. 3. Overexpression of *walR* from a multi-copy plasmid impairs growth, alters morphology and**
598 **slows autolysis in 630Δerm**. A. Viability assay. Overnight cultures of 630Δerm harboring pCE691
599 (P_{xyl}::*walR*) or the empty vector control plasmid pBZ101 (P_{xyl} EV) were serially diluted and spotted onto
600 TY-Thi plates with or without 1% xylose. Plates were photographed after incubation overnight. (B) Growth

601 curve of 630Δerm/pCE691 (P_{xyl}::*walR*). Duplicate cultures were grown to an OD_{600} of 0.2, at which time
602 one was induced with 3% xylose (green arrow). Both cultures were harvested after 3h (red arrow) for
603 analysis by phase contrast microscopy (C) and a lysis assay (D). Bar in (C) = 10 µm. For the lysis assay,
604 cells were suspended in buffer containing 0.01% Triton X-100 and OD_{600} was monitored over time. Error
605 bars depict SD of 3 technical replicates. Data shown are representative of at least 3 independent
606 experiments.
607
608 **Fig. 4. Prolonged overexpression of *walR* from a single-copy chromosomal P_{xyl}::*walR* allele**
609 **affects cell shape and slows lysis**. (A) Growth curves. An overnight culture of strain UM626 (P_{xyl}::*walR*
610 integrated at *pyrE* in 630Δerm) was subcultured 1:50 into TY with varied xylose concentrations as
611 indicated and grown for 6 hours, then analyzed in a lysis assay (B) or by phase contrast microscopy (C).
612 For the lysis assay, cells were suspended in buffer containing 0.01% Triton X-100 and OD_{600} was
613 monitored over time. Data are graphed as the mean and SD of 3 technical replicates, but most error bars
614 are smaller than the symbols. Cells from cultures grown in the presence of 0-1% xylose appeared normal
615 and are not shown, but in cultures induced with 3% xylose about 10% of the cells had irregular or bent
616 morphologies, examples of which are shown in (C). Bar = 10 µm. Data shown are representative of at
617 least 3 independent experiments.
618
619 **Fig. 5. Comparison of transcript changes between Wal-ON and Wal-OFF conditions**. (A). Heatmap
620 showing the 79 genes whose transcript abundance changed ≥ 4-fold when *walR* was overexpressed
621 (Wal-ON) in comparison to when the *wal* operon was silenced with CRISPRi (Wal-OFF). (B) Heatmap
622 showing the 49 genes whose transcript abundance changed ≥ 4-fold when the *wal* operon was silenced
623 (Wal-OFF) in comparison to when *walR* was overexpressed (Wal-ON). Green, induced. Red, repressed.
624

625 **Fig. 6. Confirmation of RNA-seq results with RFP reporter fusions to select genes.** Cells harboring
626 plasmids with transcriptional fusions of the red fluorescent protein mCherryOpt to the indicated promoters
627 were grown as per RNA-seq conditions, either Wal-ON (green) or Wal-OFF (red). Red fluorescence was
628 measured by flow cytometry and is graphed as the mean log2-fold change from two independent
629 experiments with two technical replicates. Error bars represent the SD of all four measurements. For
630 comparison, the mean log2-fold change of the same genes as determined by RNA-seq is also shown.
631 The *dltD* reporter is graphed only under Wal-OFF conditions because this fusion was induced by xylose
632 even in the absence of P_{xyl}::*walR*. Genes with asterisks denote fusions that were constructed to the
633 corresponding promoter regions from strain R20291.
634
635 **Fig. 7. Perturbation of individual Wal-ON regulon genes does not replicate the Wal-ON phenotype**.
636 Overnight cultures of 630Δerm harboring overexpression plasmids were subcultured into TY-Thi to an
637 OD_{600} of 0.03, grown to OD_{600} = 0.2 and induced with 3% xylose for 3h. Overnight cultures of 630Δerm
638 harboring CRISPRi plasmids were subcultured into TY-Thi containing 1% xylose to an OD_{600} of 0.03 and
639 grown to OD_{600} ~0.8. Each culture was then (A) examined by microscopy (bar 5 μm) and (B) tested in
640 the lysis assay. Induction of *walR* is the only condition that achieved phase bright cells and slowed lysis.
641 The plasmids used were: pBZ101 (EV), pCE691 (P_{xyl}::*walR*), pIA112 (P_{xyl}::*cd630_07380*), pIA113
642 (P_{xyl}::*cd630_07390*), pIA114 (P_{xyl}::*cd630_07380-07390*), pIA115 (P_{xyl}::*cd630_07390-07380*), pIA34
643 (sgRNA-neg), pCE744 (*sgRNA-cd630_27680-1*), and pCE745 (*sgRNA-cd630_27680-2*).
644
645 **Fig. 8. Perturbation of individual Wal-OFF regulon genes does not replicate the Wal-OFF**
646 **phenotype**. (A) Phase contrast microscopy of strains harboring overexpression plasmids or CRISPRi
647 plasmids after induction with xylose as described in the legend to Fig. 7. Bar = 5 μm. (B) Viability assay.
648 Overnight cultures were serially diluted and spotted onto TY plates with or without 1% xylose. Plates
649 were photographed after incubation overnight. CRISRPi knockdown of the *wal* operon was the only

650 condition that resulted in curved cells, lysis or a viability defect. The plasmids used were pBZ101 (EV),
651 pCE791 (P_{xyl}::*cwpV*), pIA34 (sgRNA-neg), pIA50 (sgRNA-*walA1*), and pCE738 (sgRNA-*dltD*).
652

653 **References**

654 1. Rohs PDA, Bernhardt TG. 2021. Growth and Division of the Peptidoglycan Matrix. Annu Rev Microbiol
655 75:315-336.
656 2. Fabret C, Hoch JA. 1998. A two-component signal transduction system essential for growth of *Bacillus*
657 *subtilis*: implications for anti-infective therapy. J Bacteriol 180:6375-83.
658 3. Martin PK, Li T, Sun D, Biek DP, Schmid MB. 1999. Role in cell permeability of an essential two-
659 component system in *Staphylococcus aureus*. J Bacteriol 181:3666-73.
660 4. Dubrac S, Msadek T. 2004. Identification of genes controlled by the essential YycG/YycF two-component
661 system of *Staphylococcus aureus*. J Bacteriol 186:1175-81.
662 5. Dubrac S, Boneca IG, Poupel O, Msadek T. 2007. New insights into the WalK/WalR (YycG/YycF) essential
663 signal transduction pathway reveal a major role in controlling cell wall metabolism and biofilm
664 formation in *Staphylococcus aureus*. J Bacteriol 189:8257-69.
665 6. Ng WL, Robertson GT, Kazmierczak KM, Zhao J, Gilmour R, Winkler ME. 2003. Constitutive expression of
666 PcsB suppresses the requirement for the essential VicR (YycF) response regulator in *Streptococcus*
667 *pneumoniae* R6. Mol Microbiol 50:1647-63.
668 7. Ng WL, Kazmierczak KM, Winkler ME. 2004. Defective cell wall synthesis in *Streptococcus pneumoniae*
669 R6 depleted for the essential PcsB putative murein hydrolase or the VicR (YycF) response regulator. Mol
670 Microbiol 53:1161-75.
671 8. Dubrac S, Bisicchia P, Devine KM, Msadek T. 2008. A matter of life and death: cell wall homeostasis and
672 the WalKR (YycGF) essential signal transduction pathway. Mol Microbiol 70:1307-22.
673 9. Dubrac S, Msadek T. 2008. Tearing down the wall: peptidoglycan metabolism and the WalK/WalR
674 (YycG/YycF) essential two-component system. Adv Exp Med Biol 631:214-28.
675 10. Takada H, Yoshikawa H. 2018. Essentiality and function of WalK/WalR two-component system: the past,
676 present, and future of research. Biosci Biotechnol Biochem doi:10.1080/09168451.2018.1444466:1-11.
677 11. Dobihal GS, Brunet YR, Flores-Kim J, Rudner DZ. 2019. Homeostatic control of cell wall hydrolysis by the
678 WalRK two-component signaling pathway in Bacillus subtilis. Elife 8.
679 12. Bisicchia P, Noone D, Lioliou E, Howell A, Quigley S, Jensen T, Jarmer H, Devine KM. 2007. The essential
680 YycFG two-component system controls cell wall metabolism in *Bacillus subtilis*. Mol Microbiol 65:180-
681 200.
682 13. Delauné A, Dubrac S, Blanchet C, Poupel O, Mader U, Hiron A, Leduc A, Fitting C, Nicolas P, Cavaillon JM,
683 Adib-Conquy M, Msadek T. 2012. The WalKR system controls major staphylococcal virulence genes and
684 is involved in triggering the host inflammatory response. Infect Immun 80:3438-53.
685 14. Howell A, Dubrac S, Andersen KK, Noone D, Fert J, Msadek T, Devine K. 2003. Genes controlled by the
686 essential YycG/YycF two-component system of *Bacillus subtilis* revealed through a novel hybrid regulator
687 approach. Mol Microbiol 49:1639-55.
688 15. Liu X, Gallay C, Kjos M, Domenech A, Slager J, van Kessel SP, Knoops K, Sorg RA, Zhang JR, Veening JW.
689 2017. High-throughput CRISPRi phenotyping identifies new essential genes in *Streptococcus*
690 *pneumoniae*. Mol Syst Biol 13:931.
691 16. Ng WL, Tsui HC, Winkler ME. 2005. Regulation of the pspA virulence factor and essential pcsB murein
692 biosynthetic genes by the phosphorylated VicR (YycF) response regulator in *Streptococcus pneumoniae*. J
693 Bacteriol 187:7444-59.

694 17. Delaune A, Poupel O, Mallet A, Coic YM, Msadek T, Dubrac S. 2011. Peptidoglycan crosslinking relaxation
695 plays an important role in *Staphylococcus aureus* WalKR-dependent cell viability. PLoS One 6:e17054.
696 18. Takada H, Shiwa Y, Takino Y, Osaka N, Ueda S, Watanabe S, Chibazakura T, Su'etsugu M, Utsumi R,
697 Yoshikawa H. 2018. Essentiality of WalRK for growth in *Bacillus subtilis* and its role during heat stress.
698 Microbiology (Reading) 164:670-684.
699 19. CDC. 2019. Antibiotic Resistance Threats in the United States.
700 20. Fagan RP, Albesa-Jove D, Qazi O, Svergun DI, Brown KA, Fairweather NF. 2009. Structural insights into
701 the molecular organization of the S-layer from *Clostridium difficile*. Mol Microbiol 71:1308-22.
702 21. Fagan RP, Fairweather NF. 2014. Biogenesis and functions of bacterial S-layers. Nat Rev Microbiol
703 12:211-22.
704 22. Kirk JA, Banerji O, Fagan RP. 2017. Characteristics of the *Clostridium difficile* cell envelope and its
705 importance in therapeutics. Microb Biotechnol 10:76-90.
706 23. Peltier J, Courtin P, El Meouche I, Lemee L, Chapot-Chartier MP, Pons JL. 2011. *Clostridium difficile* has
707 an original peptidoglycan structure with a high level of N-acetylglucosamine deacetylation and mainly 3-
708 3 cross-links. J Biol Chem 286:29053-62.
709 24. Nguyen HT, Wolff KA, Cartabuke RH, Ogwang S, Nguyen L. 2010. A lipoprotein modulates activity of the
710 MtrAB two-component system to provide intrinsic multidrug resistance, cytokinetic control and cell wall
711 homeostasis in *Mycobacterium*. Mol Microbiol 76:348-64.
712 25. Winkler ME, Hoch JA. 2008. Essentiality, bypass, and targeting of the YycFG (VicRK) two-component
713 regulatory system in gram-positive bacteria. J Bacteriol 190:2645-8.
714 26. Müh U, Pannullo AG, Weiss DS, Ellermeier CD. 2019. A xylose-inducible expression system and a CRISPRi-
715 plasmid for targeted knock-down of gene expression in *Clostridioides difficile*. J Bacteriol
716 doi:10.1128/jb.00711-18.
717 27. Dembek M, Barquist L, Boinett CJ, Cain AK, Mayho M, Lawley TD, Fairweather NF, Fagan RP. 2015. High-
718 throughput analysis of gene essentiality and sporulation in *Clostridium difficile*. MBio 6:e02383.
719 28. Qi LS, Larson MH, Gilbert LA, Doudna JA, Weissman JS, Arkin AP, Lim WA. 2013. Repurposing CRISPR as
720 an RNA-guided platform for sequence-specific control of gene expression. Cell 152:1173-83.
721 29. Ng YK, Ehsaan M, Philip S, Collery MM, Janoir C, Collignon A, Cartman ST, Minton NP. 2013. Expanding
722 the repertoire of gene tools for precise manipulation of the *Clostridium difficile* genome: allelic exchange
723 using *pyrE* alleles. PLoS One 8:e56051.
724 30. Fukuchi K, Kasahara Y, Asai K, Kobayashi K, Moriya S, Ogasawara N. 2000. The essential two-component
725 regulatory system encoded by *yycF* and *yycG* modulates expression of the *ftsAZ* operon in *Bacillus*
726 *subtilis*. Microbiology (Reading) 146 (Pt 7):1573-1583.
727 31. Camiade E, Peltier J, Bourgeois I, Couture-Tosi E, Courtin P, Antunes A, Chapot-Chartier MP, Dupuy B,
728 Pons JL. 2010. Characterization of Acp, a peptidoglycan hydrolase of *Clostridium perfringens* with N-
729 acetylglucosaminidase activity that is implicated in cell separation and stress-induced autolysis. J
730 Bacteriol 192:2373-84.
731 32. Neuhaus FC, Baddiley J. 2003. A continuum of anionic charge: structures and functions of D-alanyl-
732 teichoic acids in gram-positive bacteria. Microbiol Mol Biol Rev 67:686-723.
733 33. Lan CY, Igo MM. 1998. Differential expression of the OmpF and OmpC porin proteins in *Escherichia coli*
734 K-12 depends upon the level of active OmpR. J Bacteriol 180:171-4.
735 34. Smith JG, Latiolais JA, Guanga GP, Pennington JD, Silversmith RE, Bourret RB. 2004. A search for amino
736 acid substitutions that universally activate response regulators. Mol Microbiol 51:887-901.
737 35. Caspi R, Billington R, Ferrer L, Foerster H, Fulcher CA, Keseler IM, Kothari A, Krummenacker M,
738 Latendresse M, Mueller LA, Ong Q, Paley S, Subhraveti P, Weaver DS, Karp PD. 2016. The MetaCyc
739 database of metabolic pathways and enzymes and the BioCyc collection of pathway/genome databases.
740 Nucleic Acids Res 44:D471-80.

741 36. Coullon H, Rifflet A, Wheeler R, Janoir C, Boneca IG, Candela T. 2020. Peptidoglycan analysis reveals that
742 synergistic deacetylase activity in vegetative *Clostridium difficile* impacts the host response. J Biol Chem
743 295:16785-16796.
744 37. Kaus GM, Snyder LF, Müh U, Flores MJ, Popham DL, Ellermeier CD. 2020. Lysozyme Resistance in
745 *Clostridioides difficile* Is Dependent on Two Peptidoglycan Deacetylases. J Bacteriol 202.
746 38. Ammam F, Patin D, Coullon H, Blanot D, Lambert T, Mengin-Lecreulx D, Candela T. 2020. AsnB is
747 responsible for peptidoglycan precursor amidation in *Clostridium difficile* in the presence of vancomycin.
748 Microbiology (Reading) 166:567-578.
749 39. Dajkovic A, Tesson B, Chauhan S, Courtin P, Keary R, Flores P, Marlière C, Filipe SR, Chapot-Chartier MP,
750 Carballido-Lopez R. 2017. Hydrolysis of peptidoglycan is modulated by amidation of meso-
751 diaminopimelic acid and Mg(2+) in *Bacillus subtilis*. Mol Microbiol 104:972-988.
752 40. Eveland SS, Pompliano DL, Anderson MS. 1997. Conditionally lethal *Escherichia coli* murein mutants
753 contain point defects that map to regions conserved among murein and folyl poly-gamma-glutamate
754 ligases: identification of a ligase superfamily. Biochemistry 36:6223-9.
755 41. Bradshaw WJ, Roberts AK, Shone CC, Acharya KR. 2018. The structure of the S-layer of *Clostridium*
756 *difficile*. J Cell Commun Signal 12:319-331.
757 42. Layec S, Decaris B, Leblond-Bourget N. 2008. Diversity of Firmicutes peptidoglycan hydrolases and
758 specificities of those involved in daughter cell separation. Res Microbiol 159:507-15.
759 43. Ho TD, Williams KB, Chen Y, Helm RF, Popham DL, Ellermeier CD. 2014. *Clostridium difficile*
760 extracytoplasmic function sigma factor sigmaV regulates lysozyme resistance and is necessary for
761 pathogenesis in the hamster model of infection. Infect Immun 82:2345-55.
762 44. Donahue EH, Dawson LF, Valiente E, Firth-Clark S, Major MR, Littler E, Perrior TR, Wren BW. 2014.
763 *Clostridium difficile* has a single sortase, SrtB, that can be inhibited by small-molecule inhibitors. BMC
764 Microbiol 14:219.
765 45. Amoroso A, Boudet J, Berzigotti S, Duval V, Teller N, Mengin-Lecreulx D, Luxen A, Simorre JP, Joris B.
766 2012. A peptidoglycan fragment triggers β-lactam resistance in *Bacillus licheniformis*. PLoS Pathog
767 8:e1002571.
768 46. Sandhu BK, Edwards AN, Anderson SE, Woods EC, McBride SM. 2019. Regulation and Anaerobic
769 Function of the *Clostridioides difficile* β-Lactamase. Antimicrob Agents Chemother 64.
770 47. Zhou Q, Rao F, Chen Z, Cheng Y, Zhang Q, Zhang J, Guan Z, He Y, Yu W, Cui G, Qi X, Hong W. 2022. The
771 cwp66 Gene Affects Cell Adhesion, Stress Tolerance, and Antibiotic Resistance in *Clostridioides difficile*.
772 Microbiol Spectr doi:10.1128/spectrum.02704-21:e0270421.
773 48. Dhiman A, Bhatnagar S, Kulshreshtha P, Bhatnagar R. 2014. Functional characterization of WalRK: A two-
774 component signal transduction system from *Bacillus anthracis*. FEBS Open Bio 4:65-76.
775 49. Woods EC, Nawrocki KL, Suárez JM, McBride SM. 2016. The *Clostridium difficile* Dlt Pathway Is
776 Controlled by the Extracytoplasmic Function Sigma Factor σ^V in Response to Lysozyme. Infect Immun
777 84:1902-1916.
778 50. Fischer W, Rösel P, Koch HU. 1981. Effect of alanine ester substitution and other structural features of
779 lipoteichoic acids on their inhibitory activity against autolysins of *Staphylococcus aureus*. J Bacteriol
780 146:467-75.
781 51. Wecke J, Perego M, Fischer W. 1996. D-alanine deprivation of *Bacillus subtilis* teichoic acids is without
782 effect on cell growth and morphology but affects the autolytic activity. Microb Drug Resist 2:123-9.
783 52. McBride SM, Sonenshein AL. 2011. Identification of a genetic locus responsible for antimicrobial peptide
784 resistance in *Clostridium difficile*. Infect Immun 79:167-76.
785 53. Peschel A, Vuong C, Otto M, Götz F. 2000. The D-alanine residues of *Staphylococcus aureus* teichoic
786 acids alter the susceptibility to vancomycin and the activity of autolytic enzymes. Antimicrob Agents
787 Chemother 44:2845-7.

788 54. Sekulovic O, Ospina Bedoya M, Fivian-Hughes AS, Fairweather NF, Fortier LC. 2015. The *Clostridium*
789 *difficile* cell wall protein CwpV confers phase-variable phage resistance. Mol Microbiol 98:329-42.
790 55. Ransom EM, Ellermeier CD, Weiss DS. 2015. Use of mCherry Red fluorescent protein for studies of
791 protein localization and gene expression in *Clostridium difficile*. Appl Environ Microbiol 81:1652-60.
792 56. Fuchs M, Lamm-Schmidt V, Sulzer J, Ponath F, Jenniches L, Kirk JA, Fagan RP, Barquist L, Vogel J, Faber F.
793 2021. An RNA-centric global view of *Clostridioides difficile* reveals broad activity of Hfq in a clinically
794 important gram-positive bacterium. Proc Natl Acad Sci U S A 118.
795 57. Dobihal GS, Flores-Kim J, Roney IJ, Wang X, Rudner DZ. 2021. The WalR-WalK signaling pathway
796 modulates the activities of both CwlO and LytE through control of the peptidoglycan deacetylase PdaC in
797 *Bacillus subtilis*. J Bacteriol doi:10.1128/jb.00533-21:Jb0053321.
798 58. Jansen A, Türck M, Szekat C, Nagel M, Clever I, Bierbaum G. 2007. Role of insertion elements and yycFG
799 in the development of decreased susceptibility to vancomycin in *Staphylococcus aureus*. Int J Med
800 Microbiol 297:205-15.
801 59. McEvoy CR, Tsuji B, Gao W, Seemann T, Porter JL, Doig K, Ngo D, Howden BP, Stinear TP. 2013.
802 Decreased vancomycin susceptibility in Staphylococcus aureus caused by IS256 tempering of WalKR
803 expression. Antimicrob Agents Chemother 57:3240-9.
804 60. Hu J, Zhang X, Liu X, Chen C, Sun B. 2015. Mechanism of reduced vancomycin susceptibility conferred by
805 *walK* mutation in community-acquired methicillin-resistant *Staphylococcus aureus* strain MW2.
806 Antimicrob Agents Chemother 59:1352-5.
807 61. Peng H, Hu Q, Shang W, Yuan J, Zhang X, Liu H, Zheng Y, Hu Z, Yang Y, Tan L, Li S, Hu X, Li M, Rao X. 2017.
808 WalK(S221P), a naturally occurring mutation, confers vancomycin resistance in VISA strain XN108. J
809 Antimicrob Chemother 72:1006-1013.
810 62. Hu Q, Peng H, Rao X. 2016. Molecular Events for Promotion of Vancomycin Resistance in Vancomycin
811 Intermediate *Staphylococcus aureus*. Front Microbiol 7:1601.
812 63. Mesnage S, Dellarole M, Baxter NJ, Rouget JB, Dimitrov JD, Wang N, Fujimoto Y, Hounslow AM, Lacroix-
813 Desmazes S, Fukase K, Foster SJ, Williamson MP. 2014. Molecular basis for bacterial peptidoglycan
814 recognition by LysM domains. Nat Commun 5:4269.
815 64. Rice KC, Bayles KW. 2008. Molecular control of bacterial death and lysis. Microbiol Mol Biol Rev 72:85-
816 109, table of contents.
817 65. Gibson DG, Young L, Chuang RY, Venter JC, Hutchison CA, 3rd, Smith HO. 2009. Enzymatic assembly of
818 DNA molecules up to several hundred kilobases. Nat Methods 6:343-5.
819 66. Dineen SS, Villapakkam AC, Nordman JT, Sonenshein AL. 2007. Repression of *Clostridium difficile* toxin
820 gene expression by CodY. Mol Microbiol 66:206-19.
821 67. Trieu-Cuot P, Carlier C, Poyart-Salmeron C, Courvalin P. 1991. Shuttle vectors containing a multiple
822 cloning site and a lacZ alpha gene for conjugal transfer of DNA from *Escherichia coli* to gram-positive
823 bacteria. Gene 102:99-104.
824 68. Kirk JA, Fagan RP. 2016. Heat shock increases conjugation efficiency in *Clostridium difficile*. Anaerobe
825 42:1-5.
826 69. Ducret A, Quardokus EM, Brun YV. 2016. MicrobeJ, a tool for high throughput bacterial cell detection
827 and quantitative analysis. Nat Microbiol 1:16077.
828 70. Bolger AM, Lohse M, Usadel B. 2014. Trimmomatic: a flexible trimmer for Illumina sequence data.
829 Bioinformatics 30:2114-20.
830 71. Mende DR, Letunic I, Huerta-Cepas J, Li SS, Forslund K, Sunagawa S, Bork P. 2017. proGenomes: a
831 resource for consistent functional and taxonomic annotations of prokaryotic genomes. Nucleic Acids Res
832 45:D529-d534.
833 72. Caspi R, Altman T, Billington R, Dreher K, Foerster H, Fulcher CA, Holland TA, Keseler IM, Kothari A, Kubo
834 A, Krummenacker M, Latendresse M, Mueller LA, Ong Q, Paley S, Subhraveti P, Weaver DS, Weerasinghe

835 D, Zhang P, Karp PD. 2014. The MetaCyc database of metabolic pathways and enzymes and the BioCyc
836 collection of Pathway/Genome Databases. Nucleic Acids Res 42:D459-71.
837 73. Almagro Armenteros JJ, Tsirigos KD, Sonderby CK, Petersen TN, Winther O, Brunak S, von Heijne G,
838 Nielsen H. 2019. SignalP 5.0 improves signal peptide predictions using deep neural networks. Nat
839 Biotechnol 37:420-423.
840 74. Savojardo C, Martelli PL, Fariselli P, Profiti G, Casadio R. 2018. BUSCA: an integrative web server to
841 predict subcellular localization of proteins. Nucleic Acids Res 46:W459-w466.
842 75. Münch R, Hiller K, Grote A, Scheer M, Klein J, Schobert M, Jahn D. 2005. Virtual Footprint and
843 PRODORIC: an integrative framework for regulon prediction in prokaryotes. Bioinformatics 21:4187-9.
844 76. Hussain HA, Roberts AP, Mullany P. 2005. Generation of an erythromycin-sensitive derivative of
845 *Clostridium difficile* strain 630 (630Δ*erm*) and demonstration that the conjugative transposon Tn*916*ΔE
846 enters the genome of this strain at multiple sites. J Med Microbiol 54:137-41.

847

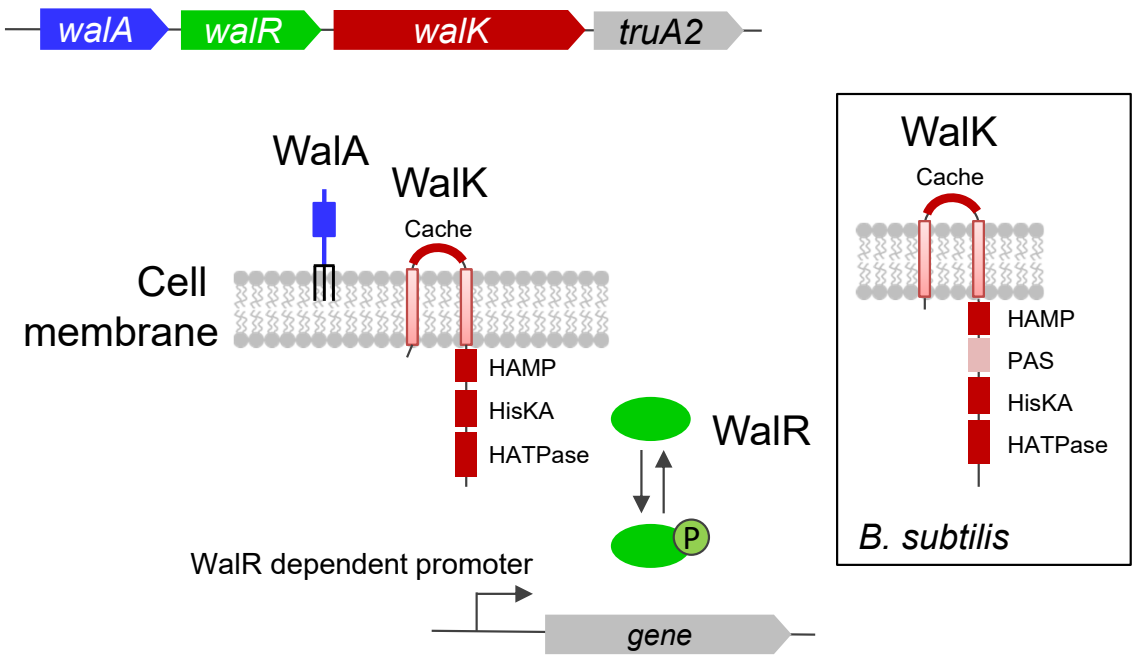

Fig. 1. The *wal* operon of *C. difficile*. Based on studies in other bacteria, WalK (red) is a bifunctional signal transducing enzyme that can phosphorylate or dephosphorylate WalR (green). WalK is predicted to have an extracellular Cache domain, as well as intracellular HAMP, HisKA (phospho-acceptor), and HATPase domains. Unlike the *B. subtilis* ortholog (inset), it does not have an intracellular PAS domain. WalR~P binds DNA to activate or repress expression of Wal-regulated genes. The lipoprotein (WalA, blue), which is unique to *C. difficile*, may modulate WalK activity and is predicted to have a beta-propeller lyase domain. The *truA2* gene codes for a pseudouridylate synthase and is not thought to play a role in Wal signaling. Operon locus: *cdr20291_1676-1679* in R20291 and *cd630_17810-17840* in 630Δerm.

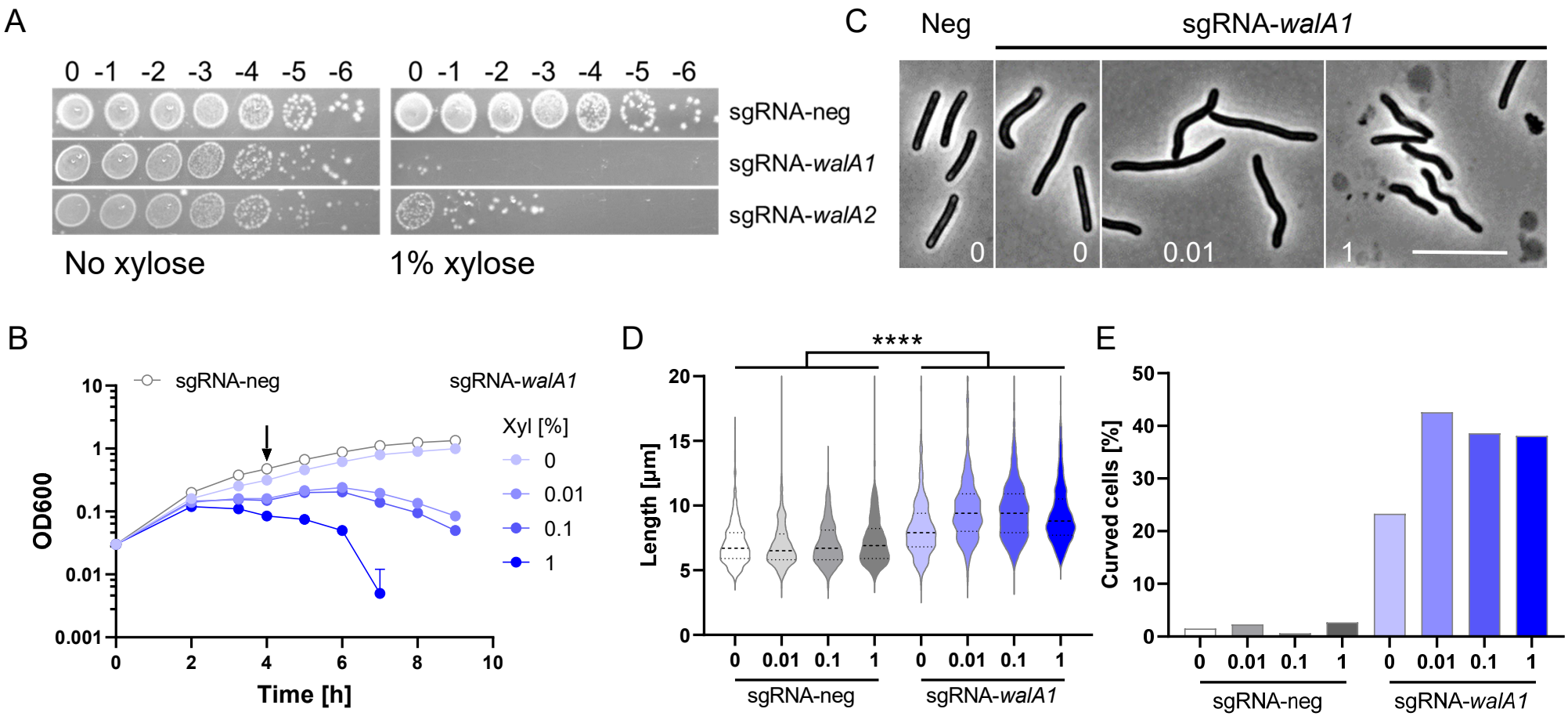

Fig. 2. The *wal* operon is required for viability and normal rod morphology of *C. difficile* 630Δerm. (A) Viability assay. Serial dilutions of overnight cultures were spotted onto TY plates with or without 1% xylose to induce the expression of *dCas9*. Plates were photographed after incubation overnight. Strains carry chromosomal copies of the CRISPRi components and the following guides: sgRNA-neg (UM554), sgRNA-*walA1* (UM555), and sgRNA-*walA2* (UM556). (B) Growth curves in liquid TY containing 0, 0.01, 0.1 or 1% xylose as indicated. For clarity, the sgRNA-neg control strain is graphed only at 0 xylose. Samples were taken at 4 hours (arrow) for phase contrast microscopy (C), cell length measurements (D) and determination of curvature (E). Numbers at the bottom of micrographs in (C) refer to % xylose. Note cell debris indicative of lysis at 1% xylose. Bar = 10 µm. Cell length and percent curved cells were based on about 500 cells per condition. The sgRNA-*walA1* strain is longer than the sgRNA-neg control in all pairwise comparisons as determined by a T-test, $p<0.0001$.

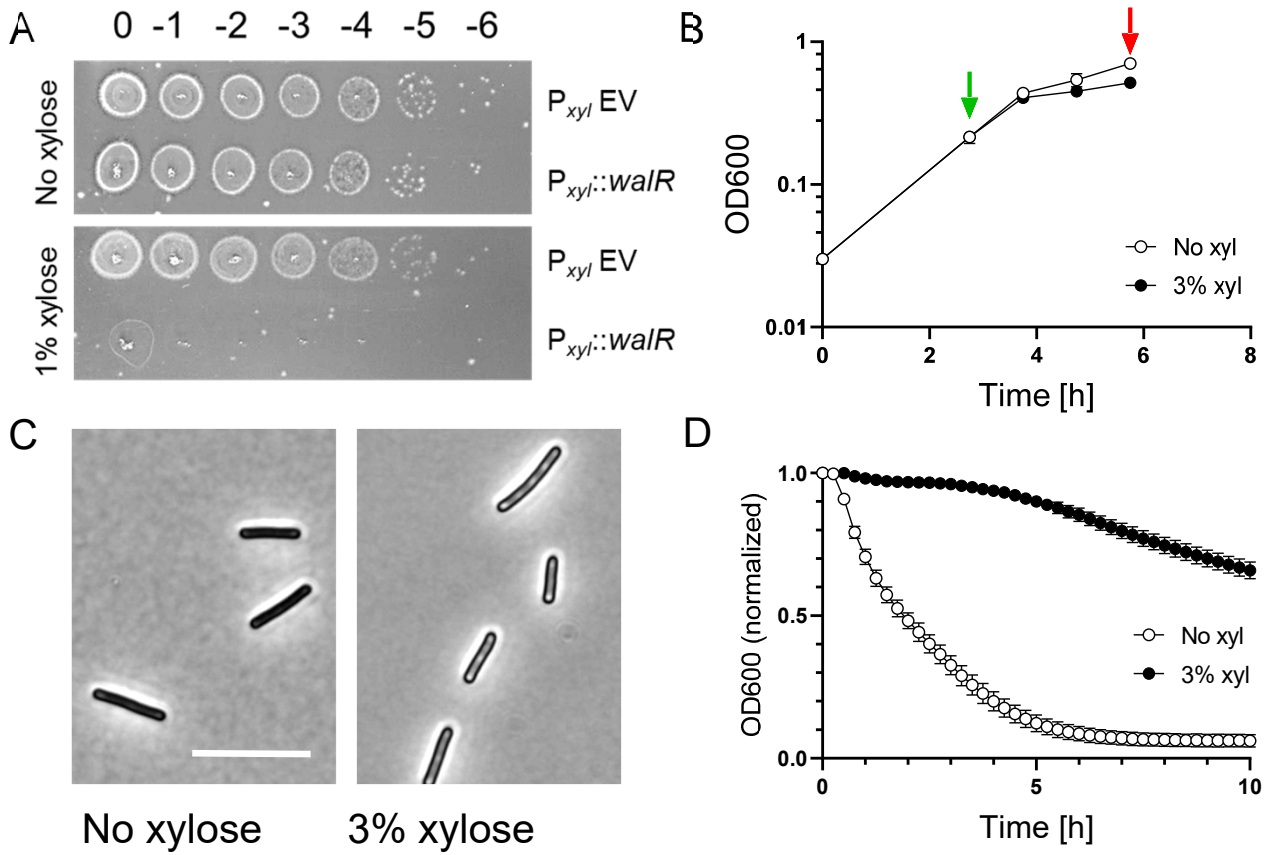

Fig. 3. Overexpression of *walR* from a multi-copy plasmid impairs growth, alters morphology and slows autolysis in 630Δerm. A. Viability assay. Overnight cultures of 630Δerm harboring pCE691 (P_{xyl}::*walR*) or the empty vector control plasmid pBZ101 (P_{xyl} EV) were serially diluted and spotted onto TY-Thi plates with or without 1% xylose. Plates were photographed after incubation overnight. (B) Growth curve of 630Δerm/pCE691 (P_{xyl}::*walR*). Duplicate cultures were grown to an OD_{600} of 0.2, at which time one was induced with 3% xylose (green arrow). Both cultures were harvested after 3h (red arrow) for analysis by phase contrast microscopy (C) and a lysis assay (D). Bar in (C) = 10 µm. For the lysis assay, cells were suspended in buffer containing 0.01% Triton X-100 and OD_{600} was monitored over time. Error bars depict SD of 3 technical replicates. Data shown are representative of at least 3 independent experiments.

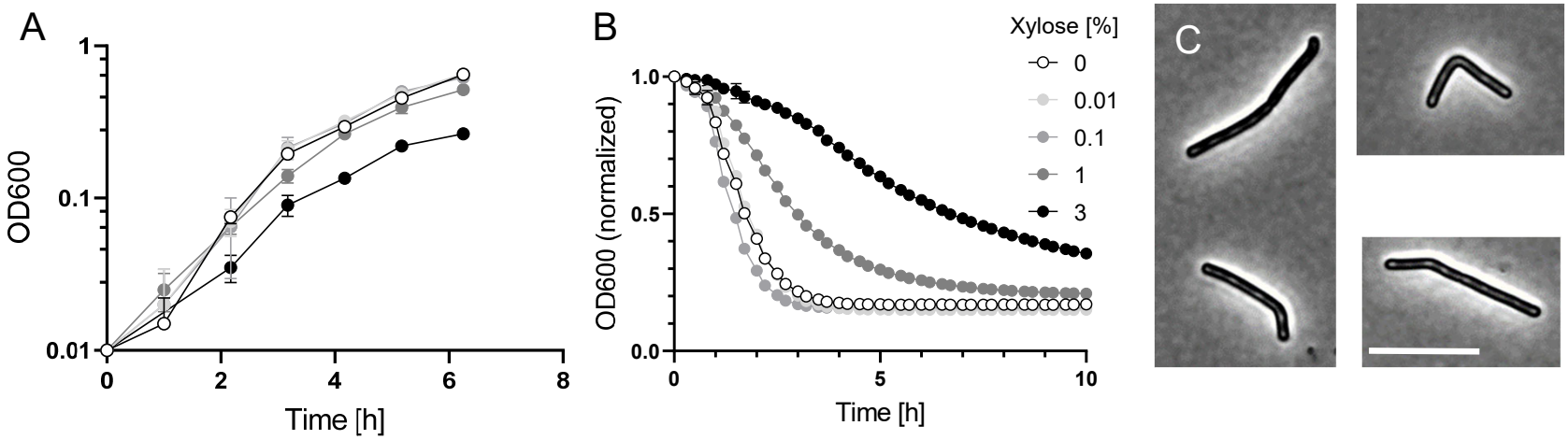

Fig. 4. Prolonged overexpression of *walR* from a single-copy chromosomal P_{xyl}::*walR* allele affects cell shape and slows lysis. (A) Growth curves. An overnight culture of strain UM626 (P_{xyl}::*walR* integrated at *pyrE* in 630Δerm) was subcultured 1:50 into TY with varied xylose concentrations as indicated and grown for 6 hours, then analyzed in a lysis assay (B) or by phase contrast microscopy (C). For the lysis assay, cells were suspended in buffer containing 0.01% Triton X-100 and OD_{600} was monitored over time. Data are graphed as the mean and SD of 3 technical replicates, but most error bars are smaller than the symbols. Cells from cultures grown in the presence of 0-1% xylose appeared normal and are not shown, but in cultures induced with 3% xylose about 10% of the cells had irregular or bent morphologies, examples of which are shown in (C). Bar = 10 µm. Data shown are representative of at least 3 independent experiments.

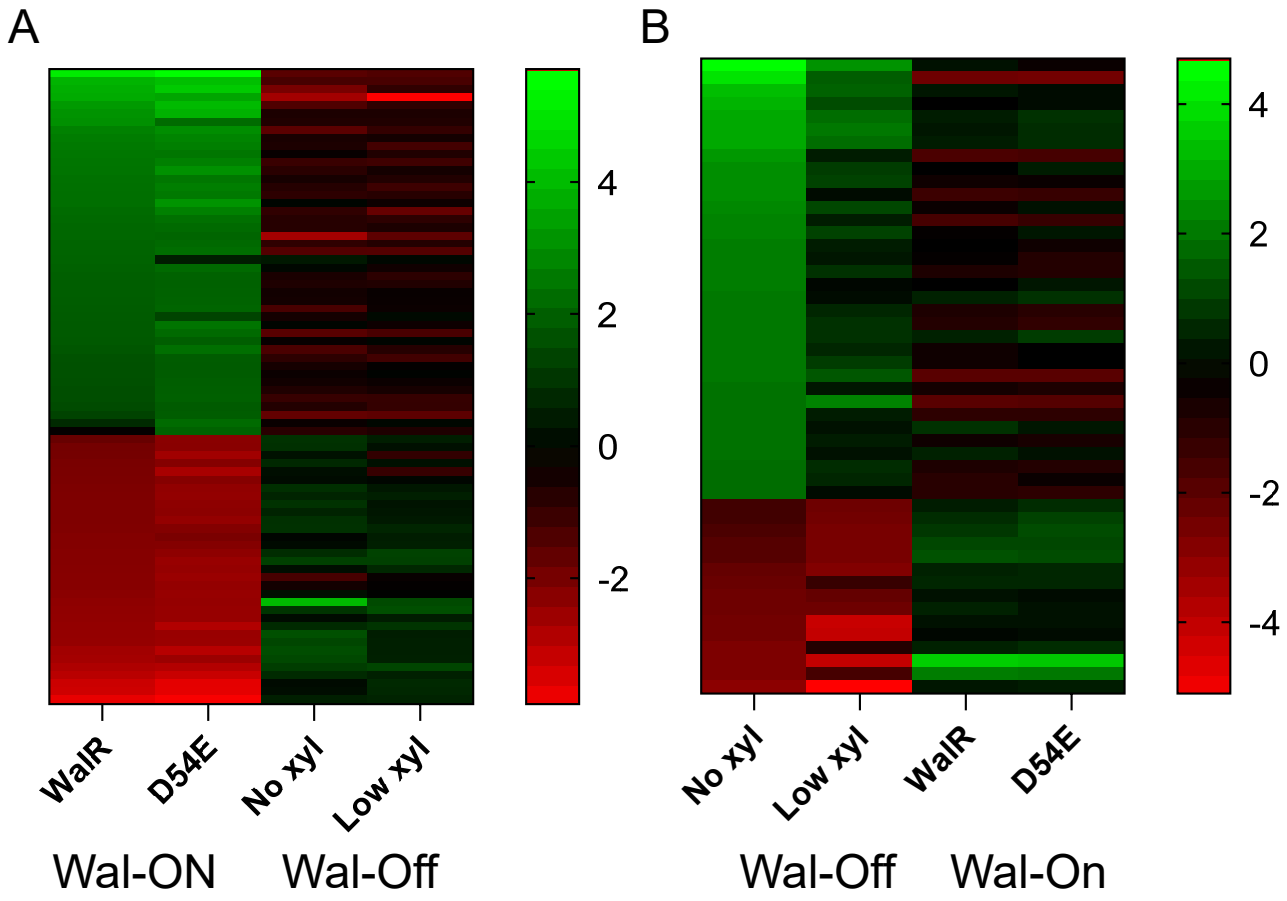

Fig. 5. Comparison of transcript changes between Wal-ON and Wal-OFF conditions. (A). Heatmap showing the 79 genes whose transcript abundance changed ≥ 4-fold when *walR* was overexpressed (Wal-ON) in comparison to when the *wal* operon was silenced with CRISPRi (Wal-OFF). (B) Heatmap showing the 49 genes whose transcript abundance changed ≥ 4-fold when the *wal* operon was silenced (Wal-OFF) in comparison to when *walR* was overexpressed (Wal-ON). Green, induced. Red, repressed.

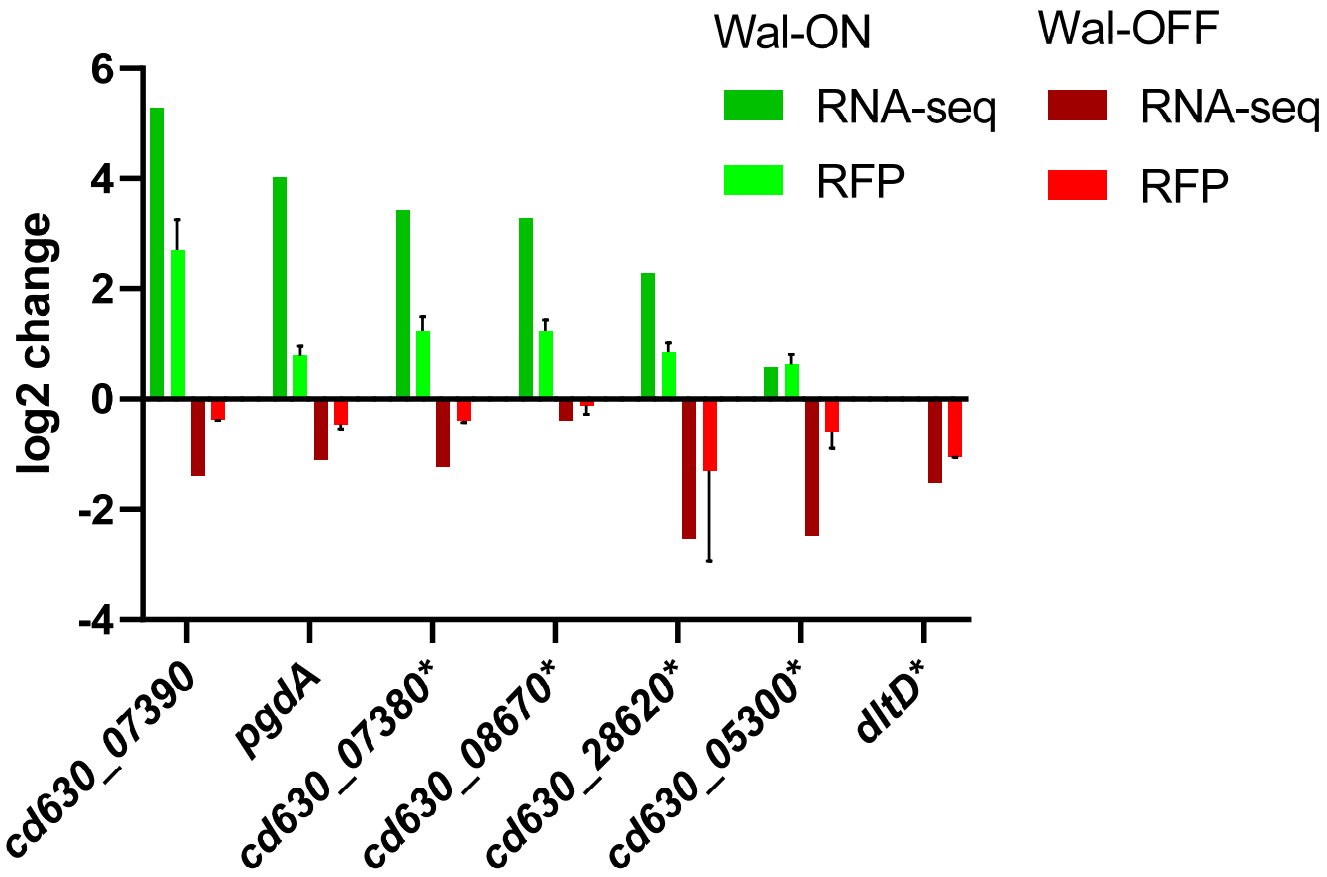

Fig. 6. Confirmation of RNA-seq results with RFP reporter fusions to select genes. Cells harboring plasmids with transcriptional fusions of the red fluorescent protein mCherryOpt to the indicated promoters were grown as per RNA-seq conditions, either Wal-ON (green) or Wal-OFF (red). Red fluorescence was measured by flow cytometry and is graphed as the mean log2-fold change from two independent experiments with two technical replicates. Error bars represent the SD of all four measurements. For comparison, the mean log2-fold change of the same genes as determined by RNA-seq is also shown. The *dltD* reporter is graphed only under Wal-OFF conditions because this fusion was induced by xylose even in the absence of P_{xyl}::*walR*. Genes with asterisks denote fusions that were constructed to the corresponding promoter regions from strain R20291.

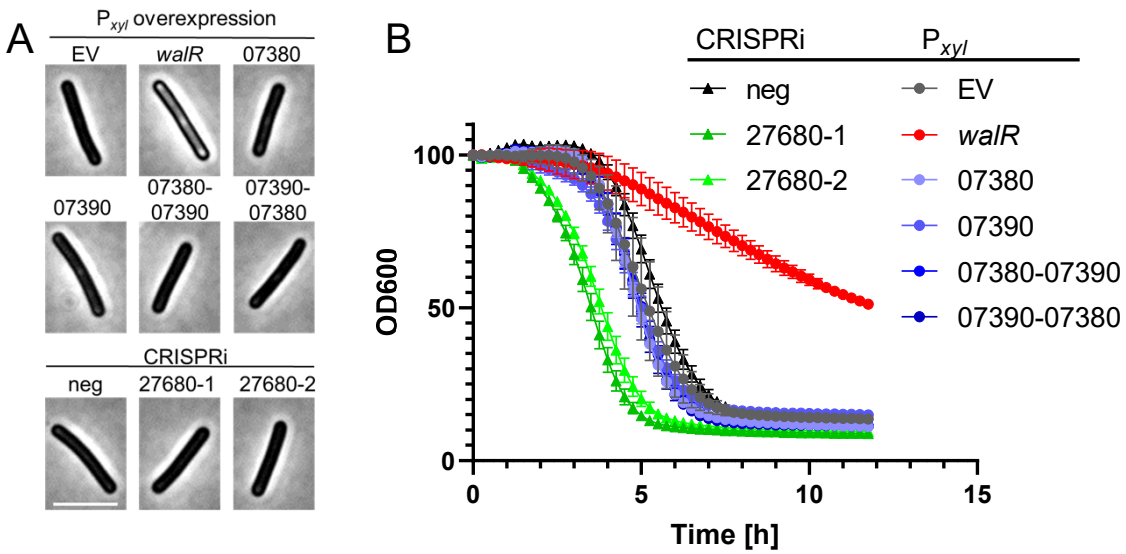

Fig. 7. Perturbation of individual Wal-ON regulon genes does not replicate the Wal-ON phenotype. Overnight cultures of 630Δerm harboring overexpression plasmids were subcultured into TY-Thi to an OD_{600} of 0.03, grown to OD_{600} = 0.2 and induced with 3% xylose for 3h. Overnight cultures of 630Δerm harboring CRISPRi plasmids were subcultured into TY-Thi containing 1% xylose to an OD_{600} of 0.03 and grown to OD_{600} ~0.8. Each culture was then (A) examined by microscopy (bar 5 µm) and (B) tested in the lysis assay. Induction of *walR* is the only condition that achieved phase bright cells and slowed lysis. The plasmids used were: pBZ101 (EV), pCE691 (P_{xyl}::*walR*), pIA112 (P_{xyl}::*cd630_07380*), pIA113 (P_{xyl}::*cd630_07390*), pIA114 (P_{xyl}::*cd630_07380-07390*), pIA115 (P_{xyl}::*cd630_07390-07380*), pIA34 (sgRNA-neg), pCE744 (*sgRNA-cd630_27680-1*), and pCE745 (*sgRNA-cd630_27680-2*).

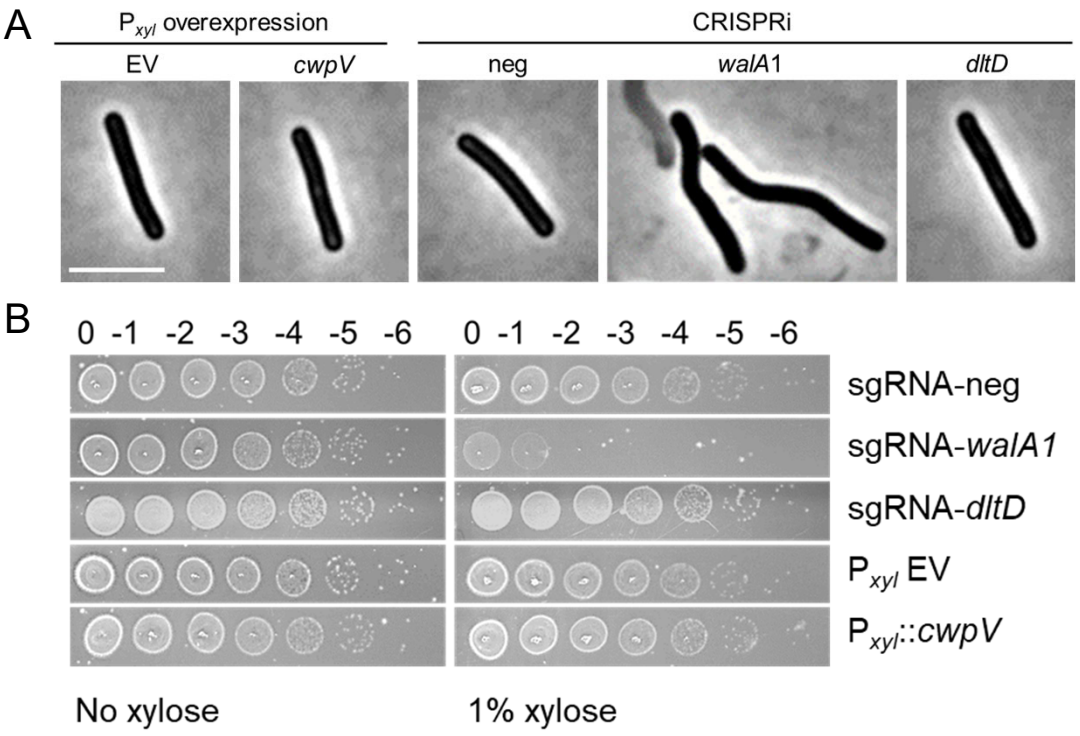

Fig. 8. Perturbation of individual Wal-OFF regulon genes does not replicate the Wal-OFF phenotype. (A) Phase contrast microscopy of strains harboring overexpression plasmids or CRISPRi plasmids after induction with xylose as described in the legend to Fig. 7. Bar = 5 μm. (B) Viability assay. Overnight cultures were serially diluted and spotted onto TY plates with or without 1% xylose. Plates were photographed after incubation overnight. CRISRPi knockdown of the *wal* operon was the only condition that resulted in curved cells, lysis or a viability defect. The plasmids used were pBZ101 (EV), pCE791 (P_{xyl}::*cwpV*), pIA34 (sgRNA-neg), pIA50 (sgRNA-*walA1*), and pCE738 (sgRNA-*dltD*).